Accepted Manuscript

Fused Heterocycles Bearing Bridgehead Nitrogen as Potent HIV-1 NNRTIs. Part 4: Design, Synthesis and Biological evaluation of Novel Imidazo[1,2-a]pyrazines

Boshi Huang, Xin Liang, Cuicui Li, Wenmin Chen, Tao Liu, Xiao Li, Yueyue Sun, Lu Fu, Huiqing Liu, Erik De Clercq, Christophe Pannecouque, Peng Zhan, Xinyong Liu

PII: S0223-5234(15)00118-X

DOI: 10.1016/j.ejmech.2015.02.022

Reference: EJMECH 7704

To appear in: *European Journal of Medicinal Chemistry*

Received Date: 29 October 2014

Revised Date: 29 January 2015

Accepted Date: 13 February 2015

Please cite this article as: B. Huang, X. Liang, C. Li, W. Chen, T. Liu, X. Li, Y. Sun, L. Fu, H. Liu, E. De Clercq, C. Pannecouque, P. Zhan, X. Liu, Fused Heterocycles Bearing Bridgehead Nitrogen as Potent HIV-1 NNRTIs. Part 4: Design, Synthesis and Biological evaluation of Novel Imidazo[1,2-a]pyrazines, European Journal of Medicinal Chemistry (2015), doi: 10.1016/j.ejmech.2015.02.022.

Graphical abstract

Through a structure-guided core-refining approach, a series of novel imidazo[1,2-*a*]pyrazine derivatives were designed, synthesized and identified as inhibitors of wild-type HIV-1 strain in this paper.

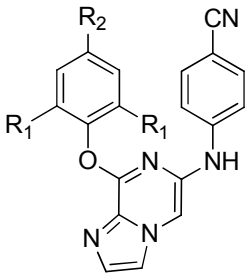

4a R_1=CH_3 R_2=CH_3 EC_{50} = 0.26 μM
5a R_1=CH_3 R_2=CN EC_{50} = 0.32 μM

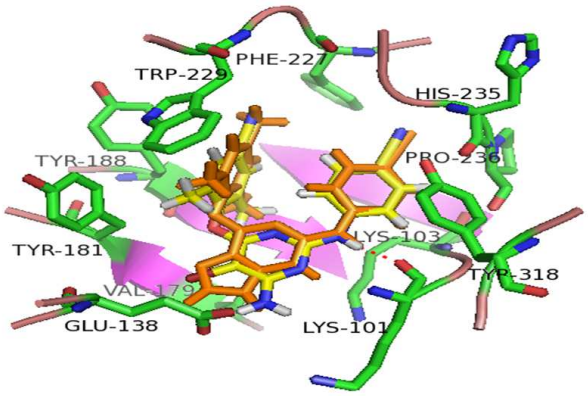

Fused Heterocycles Bearing Bridgehead Nitrogen as Potent HIV-1 NNRTIs. Part 4: Design, Synthesis and Biological evaluation of Novel Imidazo[1,2-*a*]pyrazines

Boshi Huang [a,1], Xin Liang [a,1], Cuicui Li [a], Wenmin Chen [a], Tao Liu [a], Xiao Li [a], Yueyue Sun [a], Lu Fu [a], Huiqing Liu [b], Erik De Clercq [c], Christophe Pannecouque [c], Peng Zhan [a,*], Xinyong Liu [a,*]

[a] *Department of Medicinal Chemistry, Key Laboratory of Chemical Biology (Ministry of Education), School of Pharmaceutical Sciences, Shandong University, 44 West Culture Road, 250012 Ji'nan, Shandong, PR China*

[b] *Institute of Pharmacology, School of Medicine, Shandong University, 44 West Culture Road, 250012 Ji'nan, Shandong, PR China*

[c] *Rega Institute for Medical Research, KU Leuven Minderbroedersstraat 10, B-3000 Leuven, Belgium*

Abstract: Through a structure-guided core-refining approach, a series of novel imidazo[1,2-*a*]pyrazine derivatives were designed, synthesized and evaluated as HIV-1 non-nucleoside reverse transcriptase inhibitors (NNRTIs). Biological results of antiviral assay in MT-4 cell cultures showed that 12 target compounds displayed moderate activities against wild-type (wt) HIV-1 strain (III_B) with EC_{50} values ranging from 0.26 μM to 19 μM. Among them, **4a** and **5a** were found to be the two most active analogues possessing EC_{50} values of 0.26 μM and 0.32 μM respectively, comparable to delavirdine (DLV, EC_{50} = 0.54 μM) and nevirapine (NVP, EC_{50} = 0.31 μM) in a cell-based assay. Additionally, 9 compounds showed RT inhibitory activity superior to that of NVP. Moreover, some predicted drug-like properties of

Corresponding authors. Tel: +86 531 88380270; fax: +86 531 88382731; E-mail address: zhanpeng1982@sdu.edu.cn (Zhan P.); xinyongl@sdu.edu.cn (Liu X.Y.)

1. Huang B. and Liang X. contributed equally.

representative compounds **4a** and **5a**, as well as the structure-activity relationship (SAR) analysis were discussed in detail. The binding mode of compound **4a** was investigated by molecular simulation studies.

Keywords: HIV-1 RT, Imidazo[1,2-*a*]pyrazines, Core-refining, NNRTIs, Biological activity, Molecular simulation.

1. Introduction

According to the newly released UNAIDS Gap report, there were approximately 35 million people living with HIV, 2.1 million new HIV infections and 1.5 million deaths due to AIDS in 2013[1]. In spite of the introduction of highly active antiretroviral therapy (HAART) dramatically decreasing the morbidity and mortality caused by HIV-1 infection, the AIDS prevalence remains one of the world's most serious public health problems. Owing to the excellent antiviral potency, high specificity and low cytotoxicity, HIV-1 non-nucleoside reverse transcriptase inhibitors (NNRTIs) have become inherent ingredients of HAART[2]. However, drug resistance due to reverse transcriptase (RT) mutations inevitably emerge after long-term use of NNRTIs. Thus, further development of novel inhibitors with efficient anti-HIV activity against both wild-type (wt) and mutated HIV strains, is undoubtedly required for the successful application of NNRTIs in drug combination regimens[3, 4].

Among NNRTIs, diarylpyrimidine (DAPY) derivatives with remarkable activity have attracted considerable attention over the past decade. As the most representative series of second generation NNRTIs, DAPY derivatives culminated with the US FDA's approval of Etravirine (ETR, TMC125) and Rilpivirine (RPV, TMC278) for their prominent potency against a large panel of HIV-1 mutant strains[5] (**Fig. 1**). However, most DAPY derivatives suffered from unsatisfactory pharmacokinetic profiles. For instance, the clinical advancement of ETR and RPV was hindered initially by poor aqueous solubility and bioavailability[6]. Besides, ETR proves to be an inducer of cytochrome P450 3A4 enzyme (CYP3A4), while it is an inhibitor of CYP 2C9 and CYP 2C19 on the contrary[7]. Thus, a number of drug-drug interactions must be considered when prescribing etravirine, which limits its clinical application. Taking into account these drawbacks, efforts have been focused on exploring

additional heterocyclic scaffolds as next-generation DAPY-like NNRTIs to improve pharmacokinetic and druggable properties. For instance, pyrrolopyrimidines RDEA427 and RDEA640 have been disclosed to exhibit remarkable antiviral potency against wt HIV-1 (with EC_{50} values of 0.9 and 0.8 nM, respectively) and a broad spectrum of HIV-1 mutants with low potential for CYP induction (**Fig. 2**) [8-10]. In 2014, two series of fused heterocyclic compounds bearing bridgehead nitrogen were reported by our group as DAPY-like NNRTIs . Excellent anti-HIV-1 activities were displayed by some compounds, such as pyrazolo[1,5-*a*] pyrimidine **YT-5a** (EC_{50}= 70 nM)[11] and 1,2,4-triazolo[1,5-*a*] pyrimidine **LW-7c** (EC_{50} = 50 nM)[7] (**Fig. 2**). In addition to furnishing highly potent NNRTIs, these bicyclic systems also provided additional diversification points for structure-activity relationship (SAR) studies and for improvement of the inhibitor's overall pharmaceutical properties.

The advances in structural biology further gave insights into the important interactions between the NNRTI-binding pocket (NNIBP) and the inhibitors, which could provide new guidelines for improving the subsequent structure-based molecular design of potent NNRTIs. Recently, another relatively unexplored open region termed "entrance channel" in NNIBP extending into the solvent-exposed region, which was surrounded by Leu100, Lys101, Glu138 and Val179[12], has been initially identified by Prof. W.L. Jorgensen's group. Based on the detailed inspection of the binding mode revealed by the crystallographic structure of ETR in its complex with RT, it was found that the amino and bromo groups on the central pyrimidine ring of ETR exactly pointed to the entrance channel. The amino group formed a hydrogen bond with Glu138 while the bromo group developed electrostatic interaction with Val179[13].

On the basis of this analysis, and in continuation of our pursuit of the exploitation of novel biologically potent fused heterocycles as DAPY-like NNRTIs, we designed a series of synthetically feasible imidazo[1,2-*a*]pyrazine[14] NNRTIs *via* a structure-guided core-refining approach to exploit additional interactions with the entrance channel region of NNIBP. Concretely, according to the bioisosterism principle, we employed the privileged bridgehead nitrogen heterocycle imidazo[1,2-*a*]pyrazine as the central ring of new NNRTIs, as shown in **Figure 2**.

Meanwhile, the *NH* linker connecting the central ring with the right ring, which could make a crucial hydrogen-bond interaction with the backbone of Lys101 especially in the cases of the Lys101 mutant, was maintained in view of its paramount importance. Besides, the diverse substituents (including the preponderant groups) on the left and right rings were introduced. The overall molecular conformation of DAPYs which is required for the antiviral potency should be retained. Additionally, compared to ETR, the extra imidazole ring instead of the amino and bromo groups, was installed to occupy the NNIBP entrance channel more effectively, which was expected to have potentially enhanced interactions with the key residues inside the entrance channel.

Herein, to validate these hypotheses, we reported the synthesis, *in vitro* anti-HIV potency, HIV-1 RT inhibitory activity and some predicted drug-like properties of these novel imidazo[1,2-*a*]pyrazine derivatives. The SAR and molecular simulation studies were also discussed in detail to gain further insight into this series of analogues.

2. Results and discussion

2.1. Chemistry

The synthetic route of imidazo[1,2-*a*]pyrazine derivatives as target compounds is depicted in **Scheme 1**. The intermediate 6,8-dibromoimidazo[1,2-*a*]pyrazine (**2**) was prepared from commercially available 3,5-dibromopyrazin-2-amine (**1**) by cyclizing with 2-chloroacetaldehyde[15]. Subsequently, different substituted phenols were connected to the relatively active 8-position of the fused imidazo[1,2-*a*]pyrazine ring by a nucleophilic substitution reaction in the presence of K_2CO_3[16], providing intermediates **3-8**. Finally, **3-8** underwent a $Pd(OAc)_2$-catalyzed Buchwald–Hartwig reaction[17] with corresponding anilines to yield 18 title compounds (**3a-d**, **4a-d**, **5a-d**, **6a**, **6b**, **7a**, **7b**, **8a**, **8b**). Both physicochemical and spectral data of all the synthesized compounds were found to be in full agreement with the proposed structures.

2.2. In vitro anti-HIV activity

The newly synthesized imidazo[1,2-*a*]pyrazine derivatives were tested for their anti-HIV activity in MT-4 cell cultures infected with the wt HIV-1 (strain IIIB), the double RT mutant (K103N+Y181C) HIV-1 strain (RES056), as well as HIV-2 (strain

ROD), using the MTT method as previously described. The biological results are presented as EC_{50} values, CC_{50} values and SI values as shown in **Table 1**. Zidovudine (AZT), Didanosine (DDI), Lamivudine (3TC), Nevirapine (NVP), Delavirdine mesylate (DLV), Efavirenz (EFV) and Etravirine (ETR) were used as reference drugs.

In total, 12 compounds displayed anti-HIV-1 (IIIB) activity in the micromolar range (EC_{50} = 0.26 – 19 μM) with selectivity index (SI) values ranging from 5 to ≥ 224. Among them, **4a** and **5a** were found to be the two most active analogues possessing EC_{50} values of 0.26 μM and 0.32 μM respectively, which were much lower than the reference drugs DDI (EC_{50} = 23 μM) and 3TC (EC_{50} = 2.2 μM), and comparable to DLV (EC_{50} = 0.54 μM) and NVP (EC_{50} = 0.31 μM), while much higher than for AZT (EC_{50} = 0.007 μM), EFV (EC_{50} = 0.006 μM) and ETR (EC_{50} = 0.004 μM) against IIIB strain. Compounds **4a** and **5a** also exhibited high selectivity indexes (SI = 126, ≥ 224, respectively). Also, two compounds (**7a**, EC_{50} = 0.98 μM; **8a**, EC_{50} = 0.87 μM) showed better potency than the control drugs DDI and 3TC. Unfortunately, none of the new compounds was active against the double mutant HIV-1 strain RES056 at subtoxic concentrations. Based on the anti-HIV-1 (IIIB) assay results, preliminary SAR analysis was as follows.

First of all, to elucidate the SAR profiles of the substitutents R_3, different goups were introduced on the right ring of these imidazo[1,2-*a*]pyrazine analogues, while keeping other positions unchanged. Comparing the EC_{50} and CC_{50} values of the **4a-d** sub-series characterized by a 2,4,6-trimethyl substituent on the left wing, we found that compound **4a** bearing a 4-cyano-substituent on the right ring possessed the best activity and highest SI value (SI = 126). The sequences of potency and SI values in this case indicated the same declining trend: 4-cyano > 4-nitro > 4- cyano methylene > 4-chlorine. Compounds **3a** and **5a** also showed best potency and safety profiles in the **3a-d** and **5a-d** sub-series, respectively. On the whole, 4-cyano-aniline substitution was found to be the optimal functional group for R_3 in these derivatives. The results were in agreement with those of the DAPYs previously reported.

Next, the nature of substitutions (R_1 and R_2) on the left wing was explored. Comparing the EC_{50} values of those analogues with same R_3 substituents, compounds **4a-d**, it was seen that a 2,4,6-trimethyl substituent on the left wing was most favorable to the anti-HIV-1 (IIIB) activity, superior to 2,6-dimethyl-4-cyano group and the others. Besides, by comparing compound **7a** and **8a** with **3a** (EC_{50} = 6.5 μM),

we can conclude that adding a bromine or chlorine atom at the 4-position of 2,6-dimethylphenoxy moiety was beneficial for the anti-HIV-1 potency. It was also interesting to observe the "magic methyl phenomenon": by comparing **3a** to **4a**, an additional methyl group with its lipophilic surface well buried into a hydrophobic pocket of NNIBP is anticipated to provide binding energy up to 1.5 kcal/mol, so give up to a 10-fold improvement in binding constant K_d[18] (or equivalent to EC_{50}). Certainly, a 25-fold increase for potency of **4a** (EC_{50} = 0.26 μM) over **3a** (EC_{50} = 6.5 μM) was observed . With a 2,4,6-trifluorine substituent on the left ring, **6a** exhibited the worst anti-HIV-1 profile in the 4-cyano-substituent (R_3) sub-series. In short, the decreased order of substituents on the left wing based on the antiviral activity was: 2,4,6-trimethyl (**4a**) > 2,6-dimethyl-4-cyano (**5a**) > 2,6-dimethyl-4-bromo (**7a**) ≈ 2,6-dimethyl-4-chloro (**8a**) > 2,6-dimethyl (**3a**) >2,4,6-trifluoro (**6a**).

Moreover, in the **3a-d**, **4a-d** and **5a-d** sub-series, it is noteworthy that the lowest cytotoxicity was always found in the compounds bearing cyano methylene at the R^3-position (**3c:** CC_{50} = 156 μM; **4c:** CC_{50} = 117 μM; **5c:** CC_{50} = 282 μM),

Taken together, our preliminary SAR analysis of these novel imidazo[1,2-*a*]pyrazine derivatives revealed the key structural fragments to maintain high activity against wt HIV-1: (i) The optimal moiety for the right wing was a 4-cyano-aniline group; (ii) The best group for the left wing was a 2,4,6-trimethyl-phenoxy group. (iii) Furthermore, our study revealed that the cytotoxicity was directly related to the nature of the R^3 substituent groups. Most importantly, in spite of the fact that these imidazo[1,2-*a*]pyrazines did not exhibit improved activity in comparison with ETR, they represented a novel class of anti-HIV-1 agents with great potential for further optimization. It must be said, the new imidazo[1,2-*a*]pyrazine derivatives can be readily derivatized, facilitating extensive SAR studies in the future.

Moreover, all the target compounds were also screened for their inhibition against HIV-2 (strain ROD) in MT-4 cells, but none was found effective at a subtoxic concentration, indicating that the newly synthesized compounds were only specific for HIV-1.

2.3. Inhibition of HIV-1 RT

In order to further confirm the binding target, all the compounds were tested in enzymatic assays against HIV-1 RT (WT), using poly [A] • oligo $[dT]_{15}$ as template/primer (RT kit, Roche). NVP and ETR were used as reference drugs in this assay. As shown in **Table 2**, on the whole, most compounds displayed moderate RT inhibitory activity. Among them, 9 compounds showed RT inhibitory activity superior to that of NVP. In particular, compound **5c** (IC_{50} = 0.17 μM) demonstrated the highest potency compared to that of ETR (IC_{50} = 0.13 μM). Admittedly, the enzymatic activity and SARs of these analogues exhibited some difference compared to their anti-HIV (IIIB) results, especially for cyano methylene-containing compounds **3c**, **4c** and **5c** with the recovered RT inhibition. In summary, it's reasonable that the newly synthesized imidazo[1,2-*a*]pyrazine derivatives could specifically target HIV-1 RT, and thus belonged to the class of the HIV-1 NNRTIs.

2.4. Molecular modeling analysis

Molecular modeling (docking) was performed using the Sybyl-X 1.1 software to get deeper insight into the molecular bases of the inhibitory potency and to rationalize SARs of these analogues. The most potent compound **4a** in anti-HIV-1 (IIIB) *in vitro* assay was selected to be docked into the NNIBP of HIV-1 RT (taken from the crystal structure of the RT/ETR complex, PDB entry: 3MEC).

As shown in **Figure 3**, **4a** was displayed in overlap with ETR by PyMOL version 1.5 (http://www.pymol.org/). **4a** had nearly the same binding mode as etravirine. Notable features of **4a** in the NNIBP were summarized as follows: The trimethylphenyl fitted into the aromatic-rich sub-pocket consisting of residues Tyr181, Tyr188, Phe227 and Trp229, developing positive face-to-face π–π interactions with the aromatic rings of Tyr181 and Tyr188. The right benzonitrile moiety extended to a solvent exposure region, which was surrounded by residues His235 and Pro236. Additionally, one hydrogen bond was formed between the *NH* linked to the 6-position of the core ring and the backbone carbonyl of residue Lys101. Moreover, the fused imidazole ring actually occupied the entrance channel effectively, giving rise to favorable Van der Waals interaction. However, lacking one polar interaction (like hydrogen bond interaction) between the central heterocyclic moiety and Glu138

observed in ETR may be one reason for the inferior activity of **4a**. On the whole, the modeling analysis was able to support our original design hypothesis and of the information provided above will be taken full advantage for further structural optimization.

2.5. In silico prediction of physicochemical properties

Furthermore, some physicochemical properties of **4a**, **5a** (as representative compounds) and **RDEA427**, **LW-7c**, **ETR** (as control), like LogP, molecular weight (MW), topological polar surface area (TPSA), molecular volume (MV), were determined using free on-line software (http://www.molinspiration.com/) for their compliance with the Lipinski's rule of five. The predicted results (**Table 3**) suggested that compounds **4a**, **5a** and reference compounds conformed well to the Lipinski's rule of five. In addition, imidazo[1,2-*a*]pyrazine derivatives and ETR shared similar properties. Physicochemical properties of **4a** and **5a** may not be mainly responsible for their moderate activity against wt HIV-1. In short, considering all of the results, compounds **4a** and **5a** have a better balance of moderate activity against wt HIV-1 and reasonable physicochemical properties, and thus considered as the two most promising leads for further lead optimization.

3. Conclusions

Based on the crystallographic structures of reported DAPY (or DAPY-like) analogues, a series of novel imidazo[1,2-*a*]pyrazines were designed *via* a structure-guided core-refining approach, synthesized and evaluated for their activities against wt HIV-1 (strain IIIB), K103N+Y181C double-mutated HIV-1 (strain RES056) and HIV-2 (strain ROD) in MT-4 cells. Among them, 12 compounds exhibited moderate anti-HIV-1 (IIIB) activity in micromolar range (EC_{50} = 0.26 – 19 μM). Especially, compounds **4a** and **5a** were identified as the two most active analogues in inhibiting HIV-1 possessing EC_{50} values of 0.26 μM and 0.32 μM respectively, which were much better than those of reference drugs DDI (EC_{50} = 23 μM) and 3TC (EC_{50} = 2.2 μM), comparable to DLV (EC_{50} = 0.54 μM) and NVP (EC_{50} = 0.31 μM). In addition, all the compounds were tested in enzymatic assays against HIV-1 RT (WT), and 9 compounds showed RT inhibitory activity superior to that of NVP. Furthermore, some physicochemical properties of representative compounds **4a**

and **5a** were predicted, and the results suggested that **4a** and **5a** could be considered as the two most promising leads for next-step optimization. Preliminary SARs based on anti-HIV-1 activities were discussed in detail, and molecular modeling studies performed supported our initial design hypothesis that the fused imidazole ring of new compounds could occupy the entrance channel of HIV-1 RT effectively, but lacking one polar interaction with Glu138 as observed in etravirine may be one reason for the inferior activity of this series of derivatives. These valuable information and the initial results immensely encourage us to further optimize this priviledged structure, which will be reported in due course.

4. Experimental section

4.1. Chemistry

All melting points (mp) were determined on a micromelting point apparatus and are uncorrected. Mass spectra were taken on a LC Autosampler Device: Standard G1313A instrument by electrospray ionization. ^{1}H NMR and ^{13}C NMR spectra were obtained on a Bruker AV-400 spectrometer (Bruker BioSpin, Switzerland) in the indicated solvent DMSO-d_6. Chemical shifts were expressed in δ units (ppm), using TMS as an internal reference and J values were reported in hertz (Hz). TLC was performed on Silica Gel GF254. Spots were visualized by irradiation with UV light (λ 254 nm). Flash column chromatography was performed on columns packed with silica gel 60 (200–300 mesh). Solvents were of reagent grade, and if necessary, were purified and dried by standard methods. The key reagents were purchased from commercial suppliers and not further purified when used. Rotary evaporators served in concentration of the reaction solutions under reduced pressure.

*4.1.1. General procedure for the synthesis of intermediates 6-bromo-8-substitutedphenoxy imidazo[1,2-a]pyrazines (**3**-**8**)*

6,8-Dibromoimidazo[1,2-*a*]pyrazine (**2**): 2-chloroacetaldehyde (0.79 g, 4 mmol) was slowly added to a freshly prepared solution of 3,5-dibromopyrazin-2-amine (**1**) (0.51 g, 2 mmol) in 2-propanol (20 mL). The mixture was stirred at reflux under a nitrogen atmosphere for 24 h. After cooling, CH_2Cl_2 (25 mL) and Et_3N (1 mL) were added to the reaction solution. Thereafter, the solvent was evaporated under reduced pressure, and then the residue was washed with 11 mL mixed solution (water:

2-propanol = 10:1) for 2 times, filtered and dried under vacuum to give 6,8-dibromoimidazo[1,2-*a*]pyrazine (**2**) as a brown solid, which was pure enough to be used in the next step without further purification.

6-Bromo-8-substitutedphenoxy imidazo[1,2-*a*]pyrazines (**3-8**): A mixture of appropriate substituted phenols (7 mmol) and potassium carbonate (1.93 g, 14 mmol) in 30 mL DMF was stirred for 30 min at room temperature. Then, 6,8-dibromoimidazo[1,2-*a*]pyrazine (**2**) (1.94 g, 7 mmol) was added and the mixture reacted overnight at room temperature. After the reaction was completed, 100 mL H_2O was added to the mixture. The resultant precipitate were filtered and dried in vacuo to obtain the crude products of 6-bromo-8-substitutedphenoxy imidazopyrazines (**3-8**), which could be used in the next step without further purification.

*4.1.2. General procedure for the synthesis of target compounds (**3a-d**, **4a-d**, **5a-d**, **6a**, **6b**, **7a**, **7b**, **8a**, **8b**)*

$Pd(OAc)_2$ (11.2 mg, 0.05 mmol) and Xantphos (28.9 mg, 0.05 mmol) were added to 1,4-dioxane (5 mL) in a Schlenk-type flask. After stirring for 30 min at room temperature, 6-bromo-8-substitutedphenoxy imidazo[1,2-*a*]pyrazines (**3-8**) (1 mmol), different 4-substitued anilines (1.1 mmol) and Cs_2CO_3 (651.6 mg, 2 mmol) were added to the mixture. The solution was allowed to stir at reflux under N_2 protection, and the reaction was followed by TLC until its completion. After cooling to room temperature, the reaction solution was filtered and concentrated under reduced pressure. The residue was purified by flash chromatography using proper eluant and then recrystallization to afford the target compounds **(3a-d, 4a-d, 5a-d, 6a, 6b, 7a, 7b, 8a, 8b)**.

*4.1.2.1. 4-((8-(2,6-dimethylphenoxy)imidazo[1,2-a]pyrazin-6-yl)amino)benzonitrile (**3a**)*

White solid, yield: 51%. Decomposed at 187 °C. ^{1}H NMR (400 MHz, DMSO-d_6) δ: 9.19 (s, 1H, NH), 8.18 (s, 1H, imidazole-H), 7.96 (s, 1H, pyrazine-H), 7.74 (s, 1H, imidazole-H), 7.34 (d, *J*=8.80 Hz, 2H, PhH), 7.24-7.20 (m, 3H, OPh-H), 7.08 (d, *J*=8.84 Hz, 2H, PhH), 2.11 (s, 6H, CH_3×2). ^{13}C NMR (100 MHz, DMSO-d_6) δ:

150.81, 150.09, 147.50, 137.65, 134.87, 133.22, 130.80, 130.18, 129.25, 126.25, 120.26, 117.22, 116.04, 102.28, 100.10, 16.48; ESI-MS: *m/z* 356.5 (M+1), 378.6 (M+23), $C_{21}H_{17}N_5O$ (355.14).

4.1.2.2. 8-(2,6-dimethylphenoxy)-N-(4-nitrophenyl)imidazo[1,2-a]pyrazin-6-amine ***(3b)***

Yellow solid, yield: 27%. mp: 259-261 °C. ^{1}H NMR (400 MHz, DMSO-d_6) δ: 9.62 (s, 1H, NH), 8.22 (s, 1H, imidazole-H), 8.03 (s, 1H, pyrazine-H), 7.82 (d, J=9.28 Hz, 2H, PhH), 7.77 (s, 1H, imidazole-H), 7.28-7.22 (m, 3H, OPh-H), 7.10 (d, *J*=9.28 Hz, 2H, PhH), 2.12 (s, 6H, CH_3×2). ^{13}C NMR (100 MHz, DMSO-d_6) δ: 150.87, 150.12, 149.83, 138.78, 137.22, 135.02, 130.86, 130.28, 129.25, 126.23, 125.47, 117.40, 115.13, 103.15, 16.46; ESI-MS: *m/z* 376.5 (M+1), 398.4 (M+23), $C_{20}H_{17}N_5O_3$ (375.13).

4.1.2.3.

2-(4-((8-(2,6-dimethylphenoxy)imidazo[1,2-a]pyrazin-6-yl)amino)phenyl)acetonitrile ***(3c)***

White solid, yield: 31%. mp: 98-100 °C. ^{1}H NMR (400 MHz, DMSO-d_6) δ: 8.47 (s, 1H, NH), 8.11 (d, *J*=0.52 Hz, 1H, imidazole-H), 7.84 (s, 1H, pyrazine-H), 7.68 (d, *J*=0.56 Hz, 1H, imidazole-H), 7.22-7.16 (m, 3H, OPh-H), 7.03-6.95 (m, 4H, PhH), 3.84 (s, 2H, CH_2), 2.11 (s, 6H, CH_3×2). ^{13}C NMR (100 MHz, DMSO-d_6) δ: 150.72, 150.12, 142.64, 139.44, 134.54, 130.85, 129.98, 129.14, 128.78, 126.06, 121.94, 120.03, 117.13, 116.77, 99.65, 22.02, 16.54. ESI-MS: *m/z* 370.4 (M+1), 392.4 (M+23), $C_{22}H_{19}N_5O$ (369.16).

4.1.2.4. N-(4-chlorophenyl)-8-(2,6-dimethylphenoxy)imidazo[1,2-a]pyrazin-6-amine ***(3d)***

White solid, yield: 21%. mp: 167-169 °C. ^{1}H NMR (400 MHz, DMSO-d_6) δ: 8.61 (s, 1H, NH), 8.12 (s, 1H, imidazole-H), 7.84 (s, 1H, pyrazine-H), 7.69 (s, 1H, imidazole-H), 7.24-7.18 (m, 3H, OPh-H), 7.02-6.97 (m, 4H, PhH), 2.10 (s, 6H, CH_3×2). ^{13}C NMR (100 MHz, DMSO-d_6) δ: 150.72, 150.13, 142.16, 139.15, 134.61, 130.84, 129.95, 129.19, 128.61, 126.13, 122.96, 118.15, 116.84, 99.86, 16.52. ESI-MS: *m/z* 365.4 (M+1), 367.4 (M+3), $C_{20}H_{17}ClN_4O$ (364.11).

*4.1.2.5. 4-((8-(mesityloxy)imidazo[1,2-a]pyrazin-6-yl)amino)benzonitrile (**4a**)*

White solid, yield: 28%. mp: 163-165 °C. ^{1}H NMR (400 MHz, DMSO-d_6) δ: 9.20 (s, 1H, NH), 8.17 (s, 1H, imidazole-H), 7.98 (s, 1H, pyrazine-H), 7.73 (s, 1H, imidazole-H), 7.35 (d, *J*=8.76 Hz, 2H, PhH), 7.10 (d, *J*=8.80 Hz, 2H, PhH), 7.03 (s, 2H, OPh-H), 2.32 (s, 3H, CH_3), 2.06 (s, 6H, CH_3×2). ^{13}C NMR (100 MHz, DMSO-d_6) δ: 150.97, 148.84, 147.60, 137.55, 135.12, 134.81, 133.23, 130.36, 130.27, 129.68, 120.29, 117.20, 116.07, 102.39, 100.11, 20.82, 16.43. ESI-MS: *m/z* 370.5 (M+1), 392.5 (M+23), $C_{22}H_{19}N_5O$ (369.16).

*4.1.2.6. 8-(mesityloxy)-N-(4-nitrophenyl)imidazo[1,2-a]pyrazin-6-amine (**4b**)*

Yellow solid, yield: 55%. mp: 138-140 °C. ^{1}H NMR (400 MHz, DMSO-d_6) δ: 9.60 (s, 1H, NH), 8.21 (d, *J*=0.68 Hz, 1H, imidazole-H), 8.03 (s, 1H, pyrazine-H), 7.83 (dd, *J*=7.52 Hz, *J*=1.84 Hz, 2H, PhH), 7.76 (d, *J*=0.68 Hz, 1H, imidazole-H), 7.10 (dd, *J*=7.40 Hz, *J*=2.00 Hz, 2H, PhH), 7.06 (s, 2H, OPh-H), 2.34 (s, 3H, CH_3), 2.07 (s, 6H, CH_3×2). ^{13}C NMR (100 MHz, DMSO-d_6) δ: 151.02, 149.85, 147.93, 138.76, 137.16, 135.17, 134.95, 130.46, 130.33, 129.70, 125.44, 117.38, 115.22, 103.10, 20.80, 16.39. ESI-MS: *m/z* 390.4 (M+1), 412.5 (M+23), $C_{21}H_{19}N_5O_3$ (389.15).

*4.1.2.7. 2-(4-((8-(mesityloxy)imidazo[1,2-a]pyrazin-6-yl)amino)phenyl)acetonitrile (**4c**)*

White solid, yield: 38%. mp: 185-187 °C. ^{1}H NMR (400 MHz, DMSO-d_6) δ: 8.50 (s, 1H, NH), 8.11 (s, 1H, imidazole-H), 7.84 (s, 1H, pyrazine-H), 7.68 (s, 1H, imidazole-H), 7.05-6.96 (m, 6H, OPh-H, PhH), 3.87 (s, 2H, CH_2), 2.32 (s, 3H, CH_3), 2.06 (s, 6H, CH_3×2). ^{13}C NMR (100 MHz, DMSO-d_6) δ: 150.86, 147.90, 142.58, 139.43, 135.01, 134.46, 130.40, 129.99, 129.62, 128.70, 121.90, 120.02, 117.20, 116.73, 99.43, 22.05, 20.84, 16.48. ESI-MS: *m/z* 384.4 (M+1), 406.6 (M+23), $C_{23}H_{21}N_5O$ (383.17).

*4.1.2.8. N-(4-chlorophenyl)-8-(mesityloxy)imidazo[1,2-a]pyrazin-6-amine (**4d**)*

White solid, yield: 56%. mp: 105-107 °C. ^{1}H NMR (400 MHz, DMSO-d_6) δ: 8.59 (s, 1H, NH), 8.11 (d, *J*=0.72 Hz, 1H, imidazole-H), 7.84 (s, 1H, pyrazine-H), 7.68 (d, *J*=0.72 Hz, 1H, imidazole-H), 7.04-6.98 (m, 6H, OPh-H, PhH), 2.31 (s, 3H, CH_3), 2.05 (s, 6H, CH_3×2). ^{13}C NMR (100 MHz, DMSO-d_6) δ: 150.88, 147.90, 142.19,

139.12, 134.98, 134.53, 130.40, 130.04, 129.63, 128.61, 123.01, 118.29, 116.81, 99.83, 20.82, 16.46. ESI-MS: *m/z* 379.5 (M+1), 381.4 (M+23), $C_{21}H_{19}ClN_4O$ (378.12).

4.1.2.9.

4-((6-((4-cyanophenyl)amino)imidazo[1,2-a]pyrazin-8-yl)oxy)-3,5-dimethylbenzonitrile (**5a**)

White solid, yield: 66%. decomposed at 184 °C. ^{1}H NMR (400 MHz, DMSO-d_6) δ: 9.19 (s, 1H, NH), 8.21 (d, *J*=0.84 Hz, 1H, imidazole-H), 8.03 (s, 1H, pyrazine-H), 7.79 (s, 2H, OPh-H), 7.76 (d, *J*=0.64 Hz, 1H, imidazole-H), 7.40 (d, *J*=8.84 Hz, 2H, PhH), 7.04 (d, *J*=8.84 Hz, 2H, PhH), 2.16 (s, 6H, CH_3×2). ^{13}C NMR (100 MHz, DMSO-d_6) δ: 153.92, 150.14, 147.40, 137.24, 135.18, 133.26, 133.19, 129.97, 120.22, 119.01, 117.47, 115.97, 109.11, 103.20, 100.34, 16.20. ESI-MS: *m/z* 381.5 (M+1), 403.5 (M+23), $C_{22}H_{16}N_6O$ (380.14).

4.1.2.10.

*3,5-dimethyl-4-((6-((4-nitrophenyl)amino)imidazo[1,2-a]pyrazin-8-yl)oxy)benzonitrile (**5b**)*

Yellow solid, yield: 30%. mp: 133-135 °C. ^{1}H NMR (400 MHz, DMSO-d_6) δ: 9.61 (s, 1H, NH), 8.24 (s, 1H, imidazole-H), 8.10 (s, 1H, pyrazine-H), 7.88 (d, *J*=9.28 Hz, 2H, PhH), 7.83 (s, 2H, OPh-H), 7.79 (s, 1H, imidazole-H), 7.05 (d, *J*=9.24 Hz, 2H, PhH), 2.17 (s, 6H, CH_3×2). ^{13}C NMR (100 MHz, DMSO-d_6) δ: 153.91, 150.20, 149.72, 138.90, 136.78, 135.33, 133.32, 133.19, 130.05, 125.53, 118.97, 117.66, 115.02, 109.13, 104.09, 16.19. ESI-MS: *m/z* 401.5 (M+1), 423.4 (M+23), $C_{21}H_{16}N_6O_3$ (400.13).

4.1.2.11.

*4-((6-((4-(cyanomethyl)phenyl)amino)imidazo[1,2-a]pyrazin-8-yl)oxy)-3,5-dimethylbenzonitrile (**5c**)*

White solid, yield: 19%. mp: 174-176 °C. ^{1}H NMR (400 MHz, DMSO-d_6) δ: 8.48 (s, 1H, NH), 8.13 (d, J=0.44 Hz, 1H, imidazole-H), 7.91 (s, 1H, pyrazine-H), 7.76 (s, 2H, OPh-H), 7.70 (s, 1H, imidazole-H), 7.01 (m, 4H, PhH), 3.86 (s, 2H, CH_2), 2.16 (s, 6H, CH_3×2). ^{13}C NMR (100 MHz, DMSO-d_6) δ: 153.97, 150.06, 142.45, 139.12,

134.86, 133.30, 133.06, 129.73, 128.82, 122.28, 119.94, 119.01, 117.24, 117.04, 109.02, 100.31, 22.08, 16.26. ESI-MS: *m/z* 395.4 (M+1), 417.5 (M+23), $C_{23}H_{18}N_6O$ (394.15).

4.1.2.12.

*4-((6-((4-chlorophenyl)amino)imidazo[1,2-a]pyrazin-8-yl)oxy)-3,5-dimethylbenzonitrile (**5d**)*

White solid, yield: 20%. mp: 195-197 °C. ^{1}H NMR (400 MHz, DMSO-d_6) δ: 8.63 (s, 1H, NH), 8.15 (d, *J*=0.52 Hz, 1H, imidazole-H), 7.89 (s, 1H, pyrazine-H), 7.80 (s, 2H, OPh-H), 7.72 (d, *J*=0.52 Hz, 1H, imidazole-H), 7.04-6.95 (m, 4H, PhH), 2.15 (s, 6H, CH_3×2). ^{13}C NMR (100 MHz, DMSO-d_6) δ: 154.01, 150.04, 141.95, 138.86, 134.93, 133.31, 133.14, 129.69, 128.65, 123.24, 119.05, 118.23, 117.10, 109.00, 100.53, 16.23. ESI-MS: *m/z* 390.4 (M+1), 392.4 (M+3), 412.4 (M+23), $C_{21}H_{16}ClN_5O$ (389.10).

4.1.2.13.

*4-((8-(2,4,6-trifluorophenoxy)imidazo[1,2-a]pyrazin-6-yl)amino)benzonitrile (**6a**)*

White solid, yield: 19%. decomposed at 269 °C. ^{1}H NMR (400 MHz, DMSO-d_6) δ: 9.32 (s, 1H, NH), 8.24 (s, 1H, imidazole-H), 8.11 (s, 1H, pyrazine-H), 7.80 (s, 1H, imidazole-H), 7.58 (t, $J_{H\text{-}F}$=8.64 Hz, 2H, OPh-H), 7.50 (d, *J*=8.80 Hz, 2H, PhH), 7.13 (d, *J*=8.80 Hz, 2H, PhH). ^{13}C NMR (100 MHz, DMSO-d_6) δ: 154.38, 149.51, 147.24, 136.60, 135.63, 133.43, 129.59, 120.22, 117.74, 116.00, 104.25, 102.38 (t, $J_{C\text{-}F}$=27.00 Hz, 3C, OPh-C), 100.60. ESI-MS: *m/z* 382.4 (M+1), 404.4 (M+23), $C_{19}H_{10}F_3N_5O$ (381.08).

*4.1.2.14. N-(4-nitrophenyl)-8-(2,4,6-trifluorophenoxy)imidazo[1,2-a]pyrazin-6-amine (**6b**)*

Yellow solid, yield: 16%. mp: 268-270 °C. ^{1}H NMR (400 MHz, DMSO-d_6) δ: 9.71 (s, 1H, NH), 8.28 (s, 1H, imidazole-H), 8.18 (s, 1H, pyrazine-H), 7.97 (d, *J*=9.24 Hz, 2H, PhH), 7.83 (s, 1H, imidazole-H), 7.62 (t, $J_{H\text{-}F}$=8.64 Hz, 2H, OPh-H), 7.15 (d, *J*=9.28 Hz, 2H, PhH). ^{13}C NMR (100 MHz, DMSO-d_6) δ: 160.82, 158.37 (t, $J_{C\text{-}F}$=14.00 Hz, 2C, OPh-C), 155.61 (ddd, $J_{C\text{-}F}$=248.00 Hz, $J_{C\text{-}F}$=14.00 Hz, $J_{C\text{-}F}$=6.00 Hz, 2C, OPh-C), 149.61, 139.18 (d, $J_{C\text{-}F}$=5.00 Hz, 1C, Ph-C), 136.17, 135.76, 129.72,

126.82, 125.64, 117.90, 115.07, 105.20, 102.38 (t, J_{C-F}=28.00 Hz, 1C, OPh-C). ESI-MS: *m/z* 402.4 (M+1), 424.4 (M+23), $C_{18}H_{10}F_3N_5O_3$ (401.07).

4.1.2.15.

4-((8-(4-bromo-2,6-dimethylphenoxy)imidazo[1,2-a]pyrazin-6-yl)amino)benzonitrile ***(7a)***

Light yellow solid, yield: 29%. decomposed at 268 °C. ^{1}H NMR (400 MHz, DMSO-d_6) δ: 9.20 (s, 1H, NH), 8.19 (d, *J*=0.60 Hz, 1H, imidazole-H), 7.99 (s, 1H, pyrazine-H), 7.74 (d, *J*=0.60 Hz, 1H, imidazole-H), 7.48 (s, 2H, OPh-H), 7.38 (d, *J*=8.80 Hz, 2H, PhH), 7.08 (d, *J*=8.84 Hz, 2H, PhH), 2.10 (s, 6H, CH_3×2). ^{13}C NMR (100 MHz, DMSO-d_6) δ: 150.43, 149.49, 147.45, 137.45, 135.00, 133.79, 133.22, 131.64, 130.08, 120.24, 118.33, 117.34, 116.12, 102.64, 100.26, 16.20. ESI-MS: *m/z* 436.4 (M+3), $C_{21}H_{16}BrN_5O$ (433.05).

4.1.2.16.

8-(4-bromo-2,6-dimethylphenoxy)-N-(4-nitrophenyl)imidazo[1,2-a]pyrazin-6-amine ***(7b)***

Yellow solid, yield: 32%. decomposed at 223 °C. ^{1}H NMR (400 MHz, DMSO-d_6) δ: 9.60 (s, 1H, NH), 8.22 (d, *J*=0.80 Hz, 1H, imidazole-H), 8.05 (s, 1H, pyrazine-H), 7.89 (dd, *J*=7.40 Hz, *J*=2.00 Hz, 2H, PhH), 7.77 (d, *J*=0.76 Hz, 1H, imidazole-H), 7.51 (s, 2H, OPh-H), 7.09 (dd, *J*=7.36 Hz, *J*=2.00 Hz, 2H, PhH), 2.11 (s, 6H, CH_3×2). ^{13}C NMR (100 MHz, DMSO-d_6) δ: 150.48, 149.72, 149.49, 138.87, 137.06, 135.15, 133.83, 131.65, 130.14, 125.51, 118.41, 117.51, 115.16, 103.37, 16.18. ESI-MS: *m/z* 454.3 (M+1), 456.3 (M+3), $C_{20}H_{16}BrN_5O_3$ (453.04).

4.1.2.17.

4-((8-(4-chloro-2,6-dimethylphenoxy)imidazo[1,2-a]pyrazin-6-yl)amino)benzonitrile ***(8a)***

Light yellow solid, yield: 33%, decomposed at 256 °C. ^{1}H NMR (400 MHz, DMSO-d_6) δ: 9.19 (s, 1H, NH), 8.19 (d, *J*=0.84 Hz, 1H, imidazole-H), 8.00 (s, 1H, pyrazine-H), 7.74 (d, *J*=0.68 Hz, 1H, imidazole-H), 7.38 (d, *J*=8.80 Hz, 2H, PhH), 7.35 (s, 2H, OPh-H), 7.08 (d, *J*=8.84 Hz, 2H, PhH), 2.10 (s, 6H, CH_3×2). ^{13}C NMR (100 MHz, DMSO-d_6) δ: 150.49, 148.94, 147.47, 137.41, 135.00, 133.37, 133.22,

130.09, 130.00, 128.70, 120.25, 117.34, 116.08, 102.70, 100.23, 16.30; ESI-MS: *m/z* 390.3 (M+1), 412.4 (M+23), $C_{21}H_{16}ClN_5O$ (389.10).

4.1.2.18.

8-(4-chloro-2,6-dimethylphenoxy)-N-(4-nitrophenyl)imidazo[1,2-a]pyrazin-6-amine ***(8b)***

Yellow solid, yield: 40%, mp: 184-186 °C. ^{1}H NMR (400 MHz, DMSO-d_6) δ: 9.60 (s, 1H, NH), 8.22 (s, 1H, imidazole-H), 8.05 (s, 1H, pyrazine-H), 7.88 (d, *J*=9.32 Hz, 2H, PhH), 7.77 (s, 1H, imidazole-H), 7.37 (s, 2H, OPh-H), 7.09 (d, *J*=9.28 Hz, 2H, PhH), 2.11 (s, 6H, CH_3×2). ^{13}C NMR (100 MHz, DMSO-d_6) δ: 150.55, 149.75, 148.96, 138.66, 137.04, 135.15, 133.43, 130.16, 130.09, 128.72, 125.49, 117.51, 115.14, 103.45, 16.28; ESI-MS: *m/z* 410.4 (M+1), 432.4 (M+23), $C_{20}H_{16}ClN_5O_3$ (409.09).

4.2. Biological activity evaluation

4.2.1. In vitro anti-HIV assay

Evaluation of the antiviral activity of the newly synthesized compounds against HIV-1 wt strain (IIIB), double mutant strain (RES056) and HIV-2 strain (ROD) was performed using the MTT method as previously described[19,20]. Stock solutions (10 × final concentration) of test compounds were added in 25 μL volumes to two series of triplicate wells so as to allow simultaneous evaluation of their effects on mock- and HIV-infected cells at the beginning of each experiment. Serial five-fold dilutions of test compounds were made directly in flat-bottomed 96-well microtiter trays using a Biomek 3000 robot (Beckman instruments, Fullerton, CA). Untreated control HIV- and mock-infected cell samples were included for each sample.

HIV-1 wt strain (IIIB), HIV-1 double mutant strain (RES056) or HIV-2 strain (ROD) stock (50 μL) at 100–300 $CCID_{50}$ (50% cell culture infectious dose) or culture medium was added to either the infected or mock-infected wells of the microtiter tray. Mock-infected cells were used to evaluate the effect of test compound on uninfected cells in order to assess its cytotoxicity. Exponentially growing MT-4 cells were centrifuged for 5 min at 1000 rpm and the supernatant was discarded. The MT-4 cells were resuspended at 6 × 10^5 cells/mL, and 50 μL volumes were transferred to the microtiter tray wells. Five days after infection, the viability of mock- and HIV-infected cells was examined spectrophotometrically by the MTT method. The

50% cytotoxic concentration (CC_{50}) was defined as the concentration of the tested compound that reduced the viability of the mock-infected MT-4 cells by 50%. The concentration achieving 50% protection from the cytopathic effect of the virus in infected cells was defined as the 50% effective concentration (EC_{50}).

4.2.2. HIV-1 RT inhibition assay

Inhibition of HIV-1 RT was performed by using homopolymer template/primer linked to a microtiter plate, biotin-dUTP and RT with detection by ELISA for quantifying HIV-1 RT expression. The incorporated quantities of the biotin-dUTP into the template represented the activity of HIV-1 RT. IC_{50} values corresponded to the concentration of the imidazo[1,2-*a*]pyrazine derivatives required to inhibit biotin-dUTP incorporation by 50%. The procedure for RT inhibition assay was performed as depicted in details by the kit (Roche) protocol[21]. The percentage inhibitory values were calculated by the following formula:

%Inhibition = [O.D. value without inhibitors (with RT) -O.D. value with RT and inhibitors]/[O.D. value without inhibitors (with RT)- O.D. value without RT and inhibitors].

Conflict of interest

The authors declare no conflict of interest.

Acknowledgments

The financial support from the Key Project of National Natural Science Foundation of China (NSFC) for International Cooperation Program (No. 81420108027, 30910103908), National Natural Science Foundation of China (No. 81273354, 81102320), Research Fund for the Doctoral Program of Higher Education of China (No. 20110131130005), Natural Science Foundation of Shandong Province (ZR2009CM016) and KU Leuven (GOA 10/014) is gratefully acknowledged. We thank K. Erven, K. Uyttersprot and C. Heens for technical assistance with the anti-HIV assays.

References

1. UNAIDS Gap report, 2014.

2. P. Zhan, X. Chen, D. Li, Z. Fang, E. De Clercq, X. Liu, HIV-1 NNRTIs: structural diversity, pharmacophore similarity, and implications for drug design, Med. Res. Rev. 33 (2013) E1-72.

3. P. Zhan, X. Liu, Z. Li, C. Pannecouque, E. De Clercq, Design strategies of novel NNRTIs to overcome drug resistance, Curr. Med. Chem. 16 (2009) 3903-3917.

4. D. Li, P. Zhan, E. De Clercq, X. Liu, Strategies for the design of HIV-1 non-nucleoside reverse transcriptase inhibitors: lessons from the development of seven representative paradigms, J. Med. Chem. 55 (2012) 3595-3613.

5. X. Chen, P. Zhan, D. Li, X. Liu, E. De Clercq, Recent advances in DAPYs and related analogues as HIV-1 NNRTIs, Curr. Med. Chem. 18 (2011) 359-376.

6. B. Huang, C. Li, W. Chen, T. Liu, M. Yu, L. Fu, Y. Sun, H. Liu, E. De Clercq, C. Pannecouque, J. Balzarini, P. Zhan, X. Liu, Fused heterocycles bearing bridgehead nitrogen as potent HIV-1 NNRTIs. Part 3: Optimization of [1,2,4]triazolo[1,5-*a*]pyrimidine core *via* structure-based and physicochemical property-driven approaches, Eur. J. Med. Chem. 92 (2015) 754-765.

7. L. Wang, Y. Tian, W. Chen, H. Liu, P. Zhan, D. Li, H. Liu, E. De Clercq, C. Pannecouque, X. Liu, Fused heterocycles bearing bridgehead nitrogen as potent HIV-1 NNRTIs. Part 2: Discovery of novel [1,2,4]Triazolo[1,5-*a*]pyrimidines using a structure-guided core-refining approach, Eur. J. Med. Chem. 85 (2014) 293-303.

8. J. Girardet, Y. Koh, S. Shaw, H. Kin, WO2006122003A2, 2006.

9. Raney A.; Hamatake R.; Xu W.; Girardet J.-L.; Vernier J.-M.; Yeh L.-T.; Quart B.; A Novel NNRTI Class With Potent Anti-HIV Activity Against NNRTI-Resistant Viruses, 21st International Conference on Antiviral Research Montreal, Quebec, Canada, 2008.

10. Raney A.; Hamatake R.; Xu W.; Vernier J.-M.; Girardet J.-L.; Weingarten P.; Zhou D.; Kim H.K.; Dick R.; Yeh L.-T.; Quart B. RDEA427 and RDEA640 are Novel NNRTIs with Potent Anti-HIV Activity Against NNRTI-Resistant Viruses, Fifteenth Conference on Retroviruses and Opportunistic Infections, Boston, MA, USA, 2008.

11. Y. Tian, D. Du, D. Rai, L. Wang, H. Liu, P. Zhan, E. De Clercq, C. Pannecouque,

X. Liu, Fused heterocyclic compounds bearing bridgehead nitrogen as potent HIV-1 NNRTIs. Part 1: design, synthesis and biological evaluation of novel 5,7-disubstituted pyrazolo[1,5-*a*]pyrimidine derivatives, Bioorg. Med. Chem. 22 (2014) 2052-2059.

12. M. Bollini, K.M. Frey, J.A. Cisneros, K.A. Spasov, K. Das, J.D. Bauman, E. Arnold, K.S. Anderson, W.L. Jorgensen, Extension into the entrance channel of HIV-1 reverse transcriptase--crystallography and enhanced solubility, Bioorg. Med. Chem. Lett. 23 (2013) 5209-5212.

13. E.B. Lansdon, K.M. Brendza, M. Hung, R. Wang, S. Mukund, D. Jin, G. Birkus, N. Kutty, X. Liu, Crystal structures of HIV-1 reverse transcriptase with etravirine (TMC125) and rilpivirine (TMC278): implications for drug design, J. Med. Chem. 53 (2010) 4295-4299.

14. Y. Song, P. Zhan, Q.Z. Zhang, X.Y. Liu, Privileged Scaffolds or Promiscuous Binders: A Glance of Pyrrolo[2,1-f][1,2,4]triazines and Related Bridgehead Nitrogen Heterocycles in Medicinal Chemistry, Curr. Pharm. Des. 19 (2013) 1528-1548.

15. H. Zeng, D.B. Belanger, P.J. Curran, G.W. Shipps, Jr., H. Miao, J.B. Bracken, M. Arshad Siddiqui, M. Malkowski, Y. Wang, Discovery of novel imidazo[1,2-*a*]pyrazin-8-amines as Brk/PTK6 inhibitors, Bioorg. Med. Chem. Lett. 21 (2011) 5870-5875.

16. X. Li, W. Chen, Y. Tian, H. Liu, P. Zhan, E. De Clercq, C. Pannecouque, J. Balzarini, X. Liu, Discovery of novel diarylpyrimidines as potent HIV NNRTIs *via* a structure-guided core-refining approach, Eur. J. Med. Chem. 80 (2014) 112-121.

17. W. Chen, P. Zhan, D. Rai, E. De Clercq, C. Pannecouque, J. Balzarini, Z. Zhou, H. Liu, X. Liu, Discovery of 2-pyridone derivatives as potent HIV-1 NNRTIs using molecular hybridization based on crystallographic overlays, Bioorg. Med. Chem. 22 (2014) 1863-1872.

18. I.D. Kuntz, K. Chen, K.A. Sharp, P.A. Kollman, The maximal affinity of ligands, Proceedings of the National Academy of Sciences, 96 (1999) 9997-10002.

19. C. Pannecouque, D. Daelemans, E. De Clercq, Tetrazolium-based colorimetric assay for the detection of HIV replication inhibitors: revisited 20 years later, Nature Protocols. 3 (2008) 427-434.

20. R. Pauwels, J. Balzarini, M. Baba, R. Snoeck, D. Schols, P. Herdewijn, J. Desmyter, E. De Clercq, Rapid and automated tetrazolium-based colorimetric assay for the detection of anti-HIV compounds, J. Virol. Methods. 20 (1988) 309-321.

21. K. Suzuki, B.P. Craddock, N. Okamoto, T. Kano, R.T. Steigbigel, Poly A-linked colorimetric microtiter plate assay for HIV reverse transcriptase, J. Virol. Methods. 44 (1993) 189-198.

Figure captions

Fig. 1. Structures of etravirine and rilpivirine.

Fig. 2. Design of 6,8-disubstituted imidazo[1,2-a]pyrazine derivatives as HIV-1 NNRTIs *via* a structure-guided core-refining approach.

Fig. 3. Predicted binding mode of **4a** (orange) docked into wt RT (PDB code: 3MEC) in overlap with ETR (yellow). Hydrogen bonds are indicated with dashed lines in red, and hydrogen atoms are omitted for clarity.

Tables

Table 1. *In vitro* anti-HIV-1 activity and cytotoxicity of title compounds (**3a-d**, **4a-d**, **5a-d**, **6a**, **6b**, **7a**, **7b**, **8a**, **8b**).

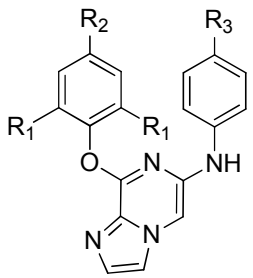

Compd	R_1	R_2	R_3	EC_{50} [a] (μM)		CC_{50} [b] (μM)	SI[c]	
				IIIB	RES056		IIIB	RES056
3a	CH_3	H	CN	6.5 ± 2.6	>32	32 ± 7.0	5	<1
3b	CH_3	H	NO_2	>5.3	nd[d]	5.3 ± 0.77	<1	nd
3c	CH_3	H	CH_2CN	>156	>156	156 ± 34	<1	<1
3d	CH_3	H	Cl	>57	>57	57 ± 65	<1	<1
4a	CH_3	CH_3	CN	0.26 ± 0.09	>33	33 ± 1.7	126	<1
4b	CH_3	CH_3	NO_2	1.3 ± 0.16	>34	34 ± 3.7	25	<1
4c	CH_3	CH_3	CH_2CN	9.2 ± 4.7	>117	117 ± 60	13	<1
4d	CH_3	CH_3	Cl	>12	>12	12 ± 6.2	<1	<1
5a	CH_3	CN	CN	0.32 ± 0.11	>73	≥73	≥224	<orX1[e]
5b	CH_3	CN	NO_2	2.3 ± 1.3	>29	29 ± 5.3	13	<1
5c	CH_3	CN	CH_2CN	19 ± 3.0	>282	282 ± 31	15	<1
5d	CH_3	CN	Cl	>13	nd	13 ± 7.1	<1	nd
6a	F	F	CN	7.2 ± 1.7	>38	38 ± 16	5	<1
6b	F	F	NO_2	>28	>28	28 ± 2.8	<1	<1
7a	CH_3	Br	CN	0.98 ± 0.18	>28	28 ± 1.5	28	<1
7b	CH_3	Br	NO_2	4.0 ± 0.46	>28	28 ± 6.1	7	<1
8a	CH_3	Cl	CN	0.87 ± 0.18	>34	34 ± 2.6	39	<1
8b	CH_3	Cl	NO_2	4.6 ± 0.54	>33	33 ± 3.0	7	<1
AZT				0.007 ± 0.002	0.01± 0.009	>94	>13144	>9149
DDI				23 ± 7.6	nd	>212	>9	nd
3TC				2.2 ± 0.82	nd	>87	>39	nd
NVP				0.31 ± 0.06	≥7.6	>15	48	>orX2
DLV				0.54 ± 0.51	>36	>36	>67	X1
EFV				0.006 ± 0.002	0.16 ± 0.01	>6.3	>1014	>41
ETR				0.004± 0.0002	0.02 ± 0.003	>4.6	>1127	>184

[a] EC_{50}: concentration of compound required to achieve 50% protection of MT-4 cells against HIV-1-induced cytopathicity, as determined by the MTT method.

[b] CC_{50}: concentration required to reduce the viability of mock-infected cells by 50%, as determined by the MTT method.

[c] SI: selectivity index (CC_{50}/EC_{50}).

[d] nd: not determined.

[e] X1: stands for ≥1 or <1.

Table 2. Inhibitory activity of target compounds, NVP and ETR against HIV-1 RT (WT)

Compd	IC_{50}[a] (μM)	Compd	IC_{50}[a] (μM)
3a	0.82	**5c**	0.17
3b	334	**5d**	5.5
3c	5.7	**6a**	0.47
3d	15	**6b**	11

4a	0.40	**7a**	0.41
4b	4.7	**7b**	4.1
4c	0.36	**8a**	1.1
4d	5.9	**8b**	1.3
5a	0.26	**NVP**	2.4
5b	14	**ETR**	0.13

[a] IC_{50}: The inhibitory concentration of the tested compounds required to inhibit biotin deoxyuridine triphosphate (biotin-dUTP) incorporation into the HIV-1 RT by 50%.

Table 3. Prediction of physicochemical properties[a] of **4a**, **5a** and reference compounds.

Compd	EC_{50} (μM)	nViol	natoms	miLogP	MW	nON	nOHNH	nrotb	TPSA	MV
Accepted range				<5	<500 Da	<10	<5	≤10	< 140 $Å^2$	
4a	0.26	1	28	5.35	369.43	6	1	4	75.25	335.84
5a	0.32	0	29	4.66	380.41	7	1	4	99.04	336.14
RDEA427	0.0009	1	29	5.00	380.41	7	2	4	110.42	335.75
LW-7c	0.05	1	28	5.01	370.42	7	1	4	88.14	331.68
ETR	0.004	1	28	5.03	435.28	7	3	4	120.65	335.95

[a] nViol = number of violations; natoms = no. of atoms; miLogP = molinspiration predicted LogP; MW= molecular weight; nON = no. of hydrogen bond acceptors; nOHNH = no. of hydrogen bond donors; nrotb = no. of rotatable bonds; TPSA = topological polar surface area; MV = molar volume.

Figures

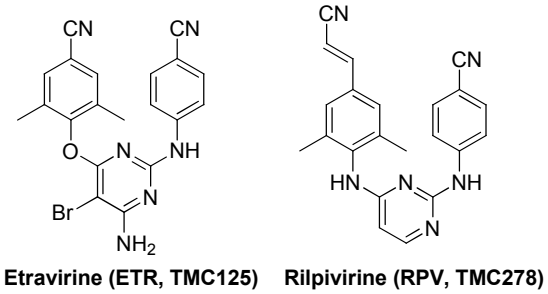

Fig. 1. Structures of etravirine and rilpivirine

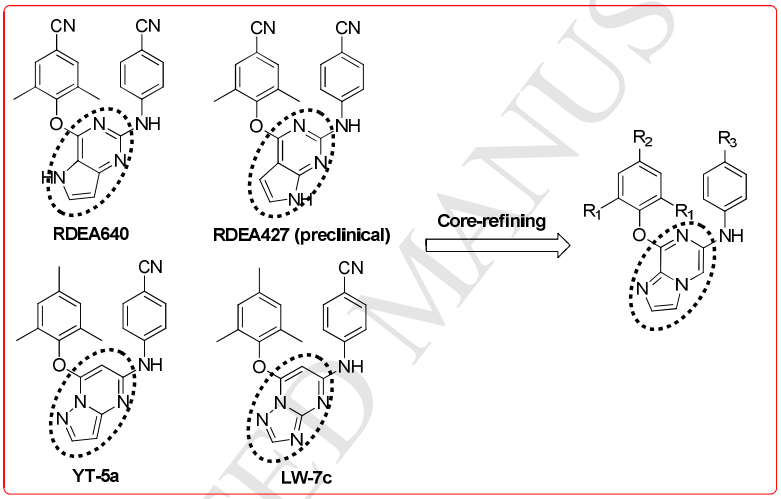

Fig. 2. Design of 6,8-disubstituted imidazo[1,2-a]pyrazine derivatives as HIV-1 NNRTIs *via* a structure-guided core-refining approach.

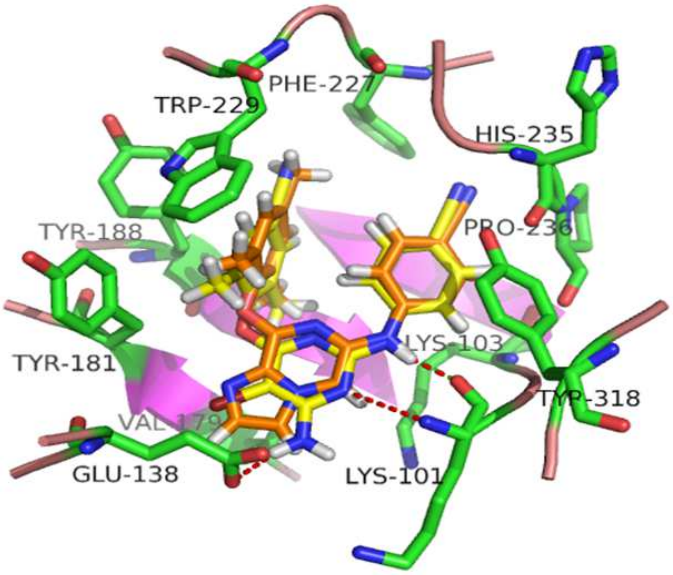

Fig. 3. Predicted binding mode of **4a** (orange) docked into wt RT (PDB code: 3MEC) in overlap with ETR (yellow). Hydrogen bonds are indicated with dashed lines in red, and hydrogen atoms are omitted for clarity.

Schemes

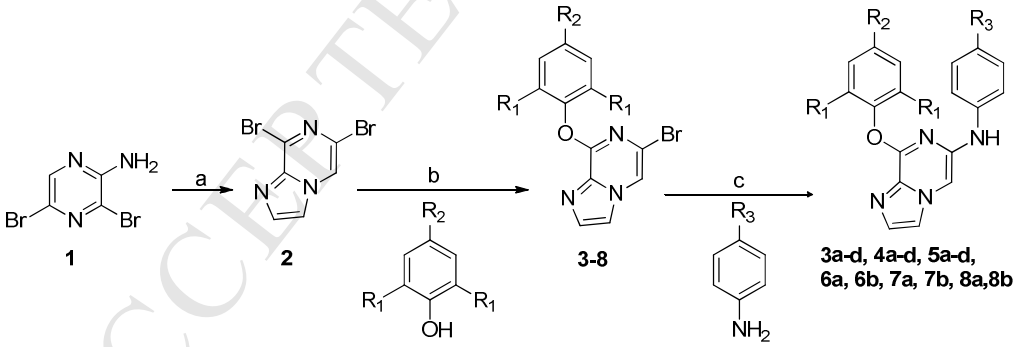

Scheme 1. The synthetic route for imidazo[1,2-*a*]pyrazine derivatives. Reagents and conditions: (a) $ClCH_2CHO$, 2-propanol, reflux in N_2 atmosphere, 24 h; (b) ArOH, K_2CO_3, DMF, r.t., overnight; (c) $ArNH_2$, $Pd(OAc)_2$, Xanphos, Cs_2CO_3, 1,4-dioxane, reflux in N_2 atmosphere.

Highlights

·Novel imidazo[1,2-*a*]pyrazines were identified as HIV-1 inhibitors.

·**4a** and **5a** exhibited anti-HIV-1 (III_B) activity with EC_{50} values of 0.26 μM and 0.32 μM respectively.

·Some drug-like properties of **4a** and **5a** were predicted.

·Preliminary SARs and molecular simulation of these new analogues were detailed.

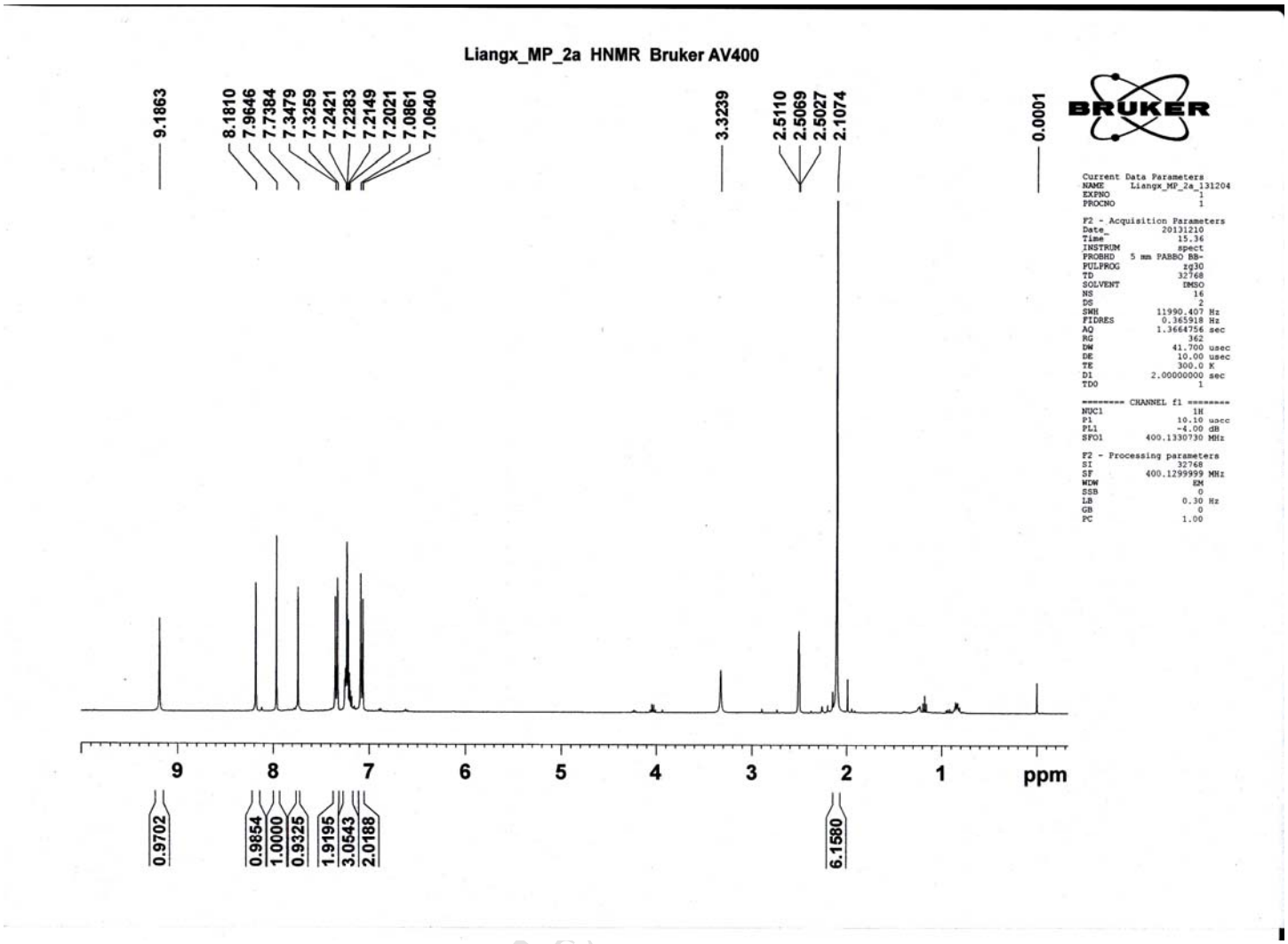
Liangx_MP_2a HNMR Bruker AV400
9.1863
8.1810
7.9646
7.7384
7.3479
7.3259
7.2421
7.2283
7.2149
7.2021
7.0861
7.0640
3.3239
2.5110
2.5069
2.5027
2.1074
0.0001
BRUKER
Current Data Parameters
NAME Liangx_MP_2a_131204
EXPNO 1
PROCNO 1
F2 - Acquisition Parameters
Date_ 20131210
Time 15.36
INSTRUM spect
PROBHD 5 mm PABBO BB-
PULPROG zg30
TD 32768
SOLVENT DMSO
NS 16
DS 2
SWH 11990.407 Hz
FIDRES 0.365918 Hz
AQ 1.3664756 sec
RG 362
DW 41.700 usec
DE 10.00 usec
TE 300.0 K
D1 2.00000000 sec
TD0 1
======== CHANNEL f1 ========
NUC1 1H
P1 10.10 usec
PL1 -4.00 dB
SFO1 400.1330730 MHz
F2 - Processing parameters
SI 32768
SF 400.1299999 MHz
WDW EM
SSB 0
LB 0.30 Hz
GB 0
PC 1.00
9
8
7
6
5
4
3
2
1
ppm
0.9702
0.9854
1.0000
0.9325
1.9195
3.0543
2.0188
6.1580

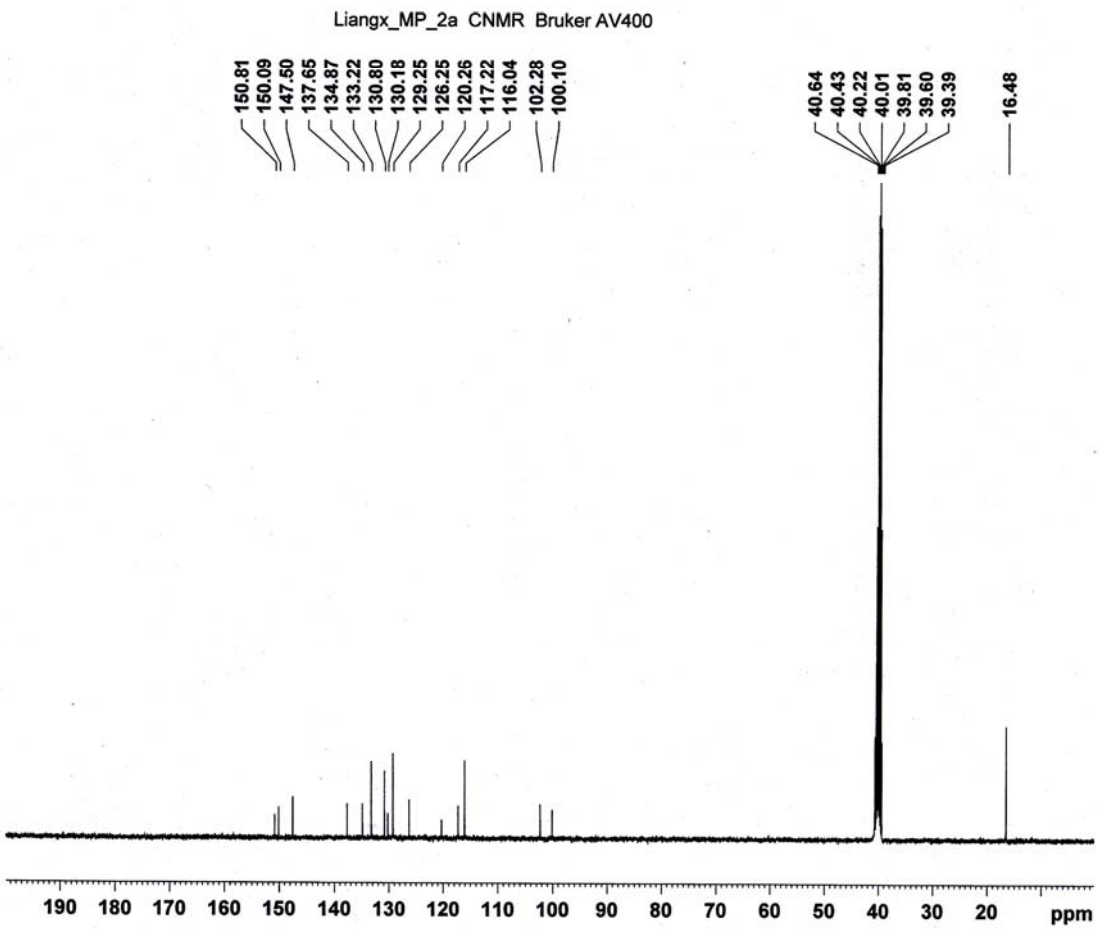

BRUKER

```
Current Data Parameters
NAME      Liangx_MP_2a_131204
EXPNO                       2
PROCNO                      1

F2 - Acquisition Parameters
Date_              20131210
Time                  16.18
INSTRUM               spect
PROBHD   5 mm PABBO BB-
PULPROG           zgpg30
TD                 65536
SOLVENT             DMSO
NS                    955
DS                      4
SWH           23980.814 Hz
FIDRES        0.365918 Hz
AQ            1.3664756 sec
RG               14596.5
DW               20.850 usec
DE                6.00 usec
TE                300.0 K
D1            2.00000000 sec
d11           0.03000000 sec
DELTA         1.89999998 sec
TD0                    12

======== CHANNEL f1 ========
NUC1                  13C
P1                 8.30 usec
PL1                -3.00 dB
SFO1         100.6228298 MHz

======== CHANNEL f2 ========
CPDPRG2          waltz16
NUC2                  1H
PCPD2             80.00 usec
PL12              12.93 dB
PL13              12.80 dB
PL2               -1.00 dB
SFO2         400.1316005 MHz

F2 - Processing parameters
SI                 32768
SF         100.6127690 MHz
WDW                   EM
SSB                    0
LB                  1.00 Hz
GB                     0
PC                  1.40
```

Corresponding to compound 3a (MS)

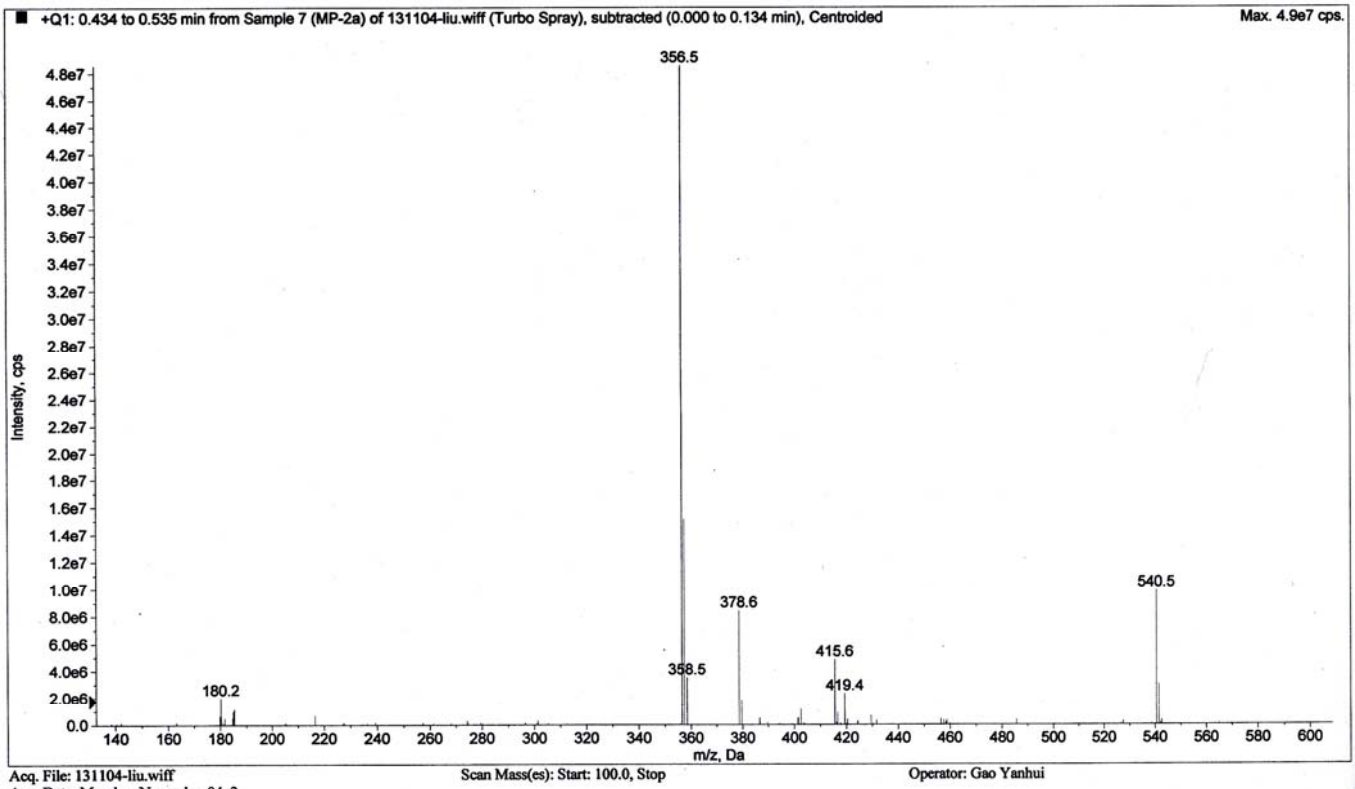

Corresponding to compound 3d (HNMR)

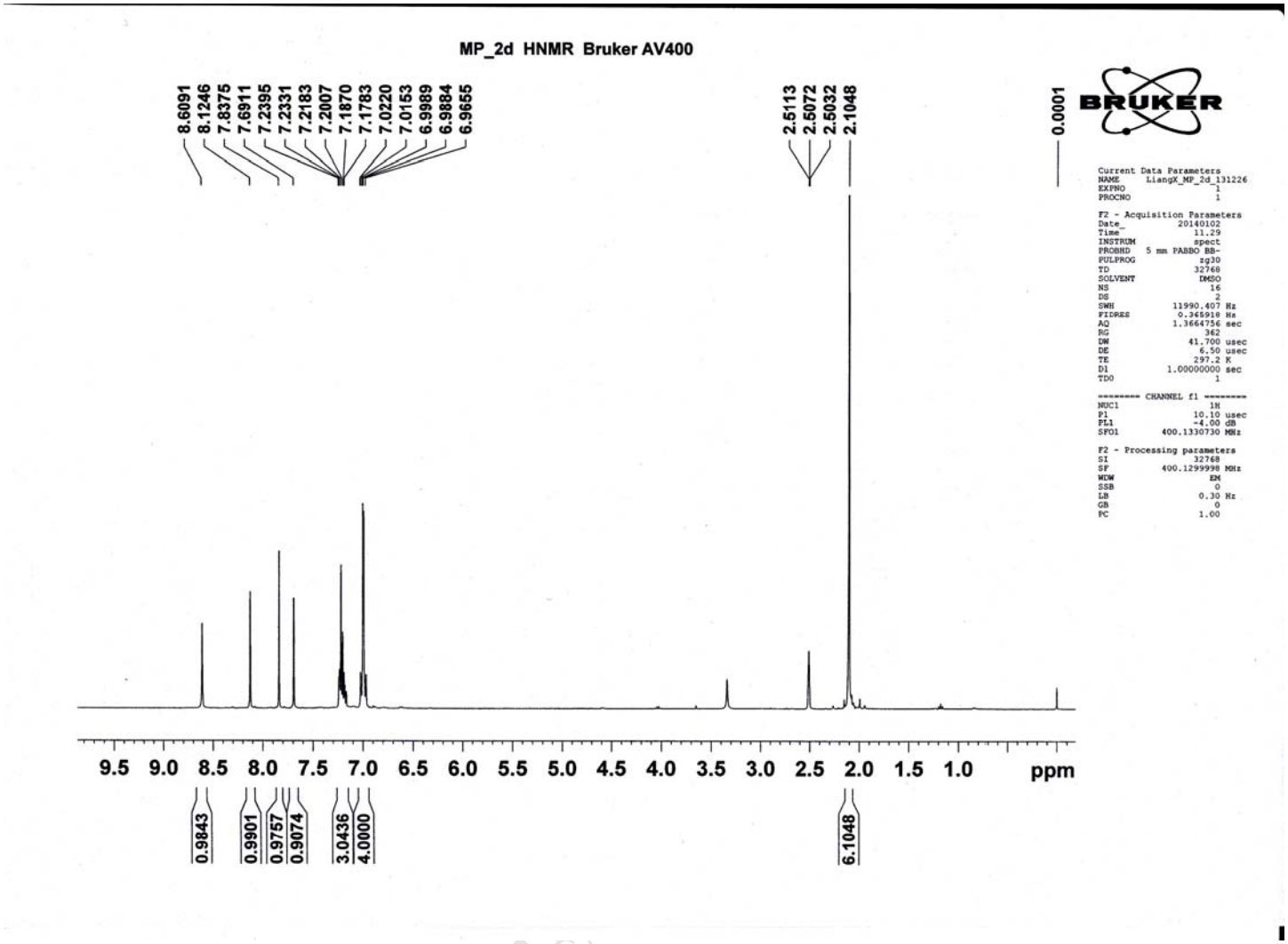

Corresponding to compound 3d (CNMR)

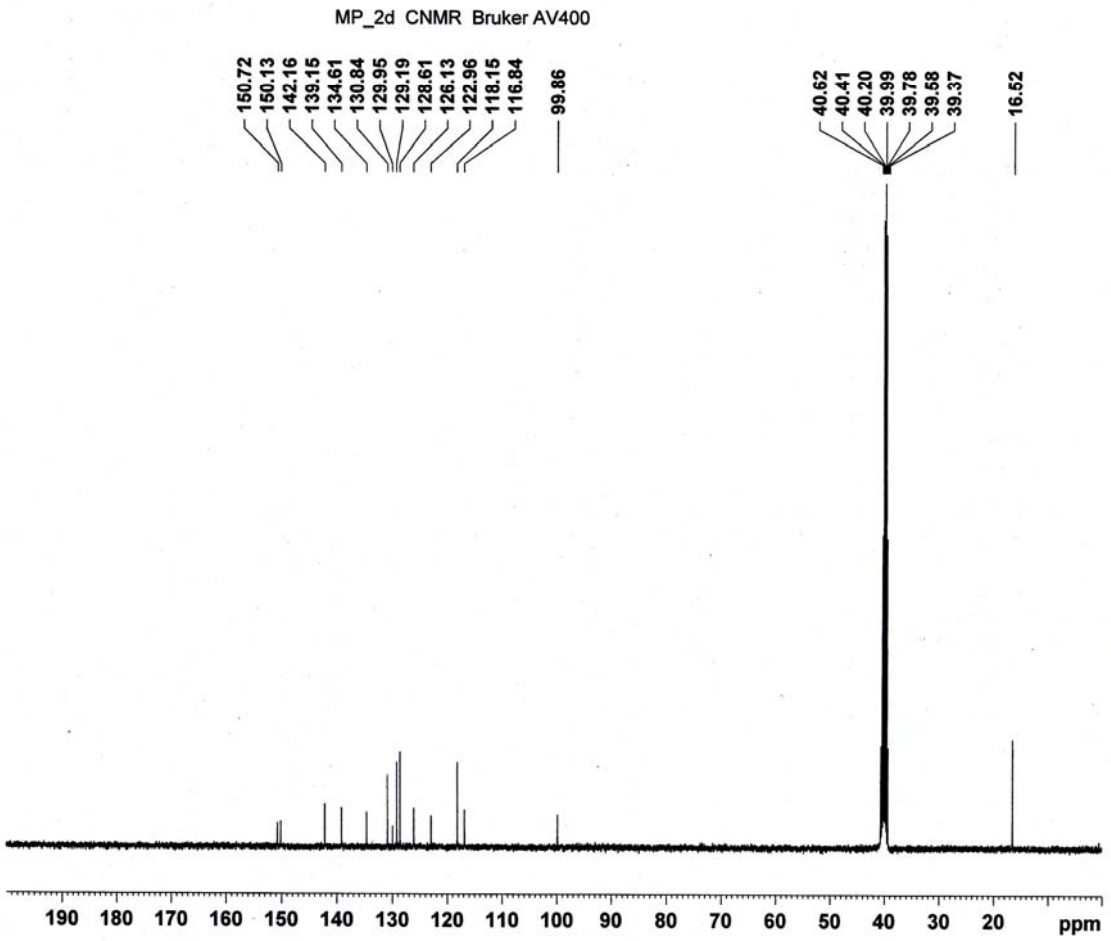

BRUKER

```
Current Data Parameters
NAME      LiangX_MP_2d_131226
EXPNO                       2
PROCNO                      1

F2 - Acquisition Parameters
Date_              20140102
Time                 11.28
INSTRUM              spect
PROBHD   5 mm PABBO BB-
PULPROG            zgpg30
TD                  65536
SOLVENT              DMSO
NS                     602
DS                       4
SWH              23980.814 Hz
FIDRES           0.365918 Hz
AQ               1.3664756 sec
RG                 20642.5
DW                  20.850 usec
DE                   8.00 usec
TE                  297.6 K
D1               2.00000000 sec
d11              0.03000000 sec
DELTA            1.89999998 sec
TD0                      8

======== CHANNEL f1 ========
NUC1                   13C
P1                    8.30 usec
PL1                  -3.00 dB
SFO1          100.6228298 MHz

======== CHANNEL f2 ========
CPDPRG2             waltz16
NUC2                    1H
PCPD2                80.00 usec
PL12                 12.93 dB
PL13                 12.80 dB
PL2                  -1.00 dB
SFO2          400.1316005 MHz

F2 - Processing parameters
SI                     32768
SF            100.6127690 MHz
WDW                    EM
SSB                     0
LB                   1.00 Hz
GB                      0
PC                   1.40
```

Corresponding to compound 3d (MS)

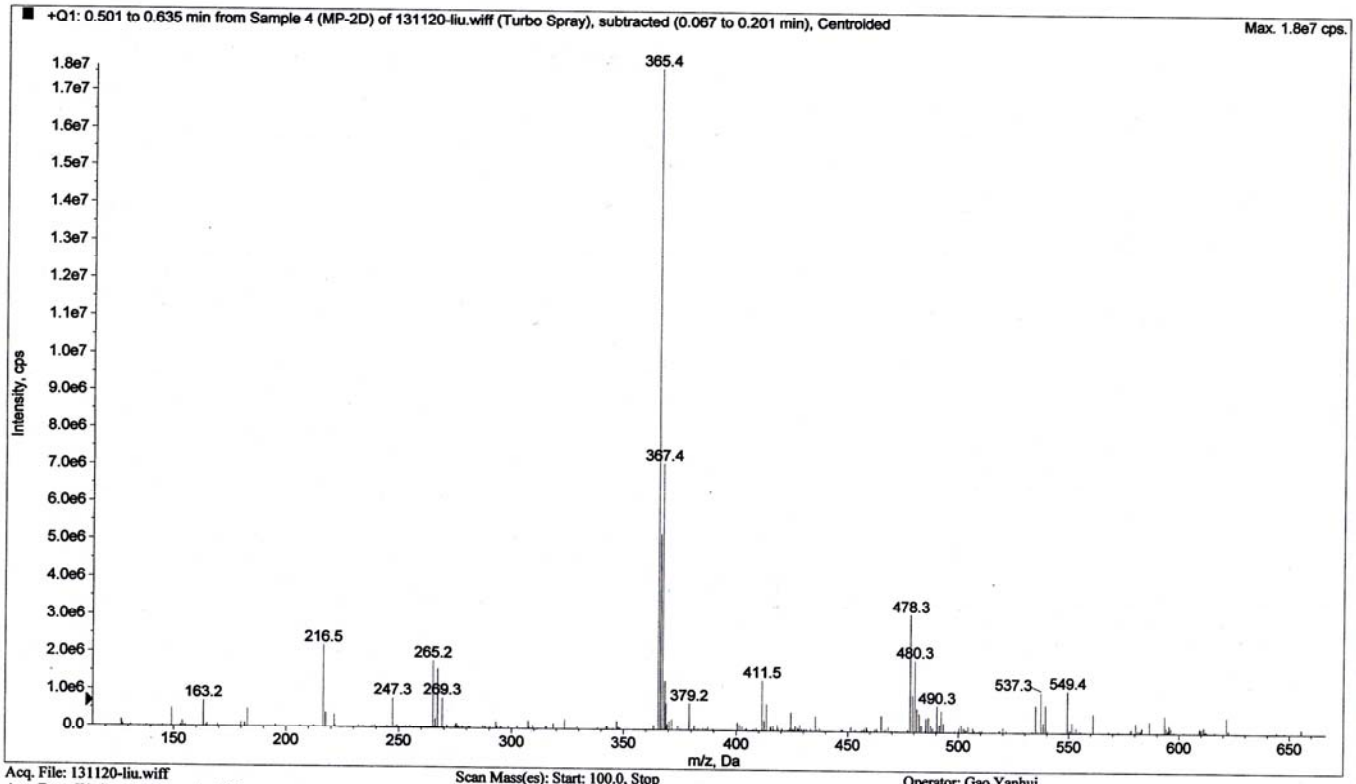

Corresponding to compound 5a (HNMR)

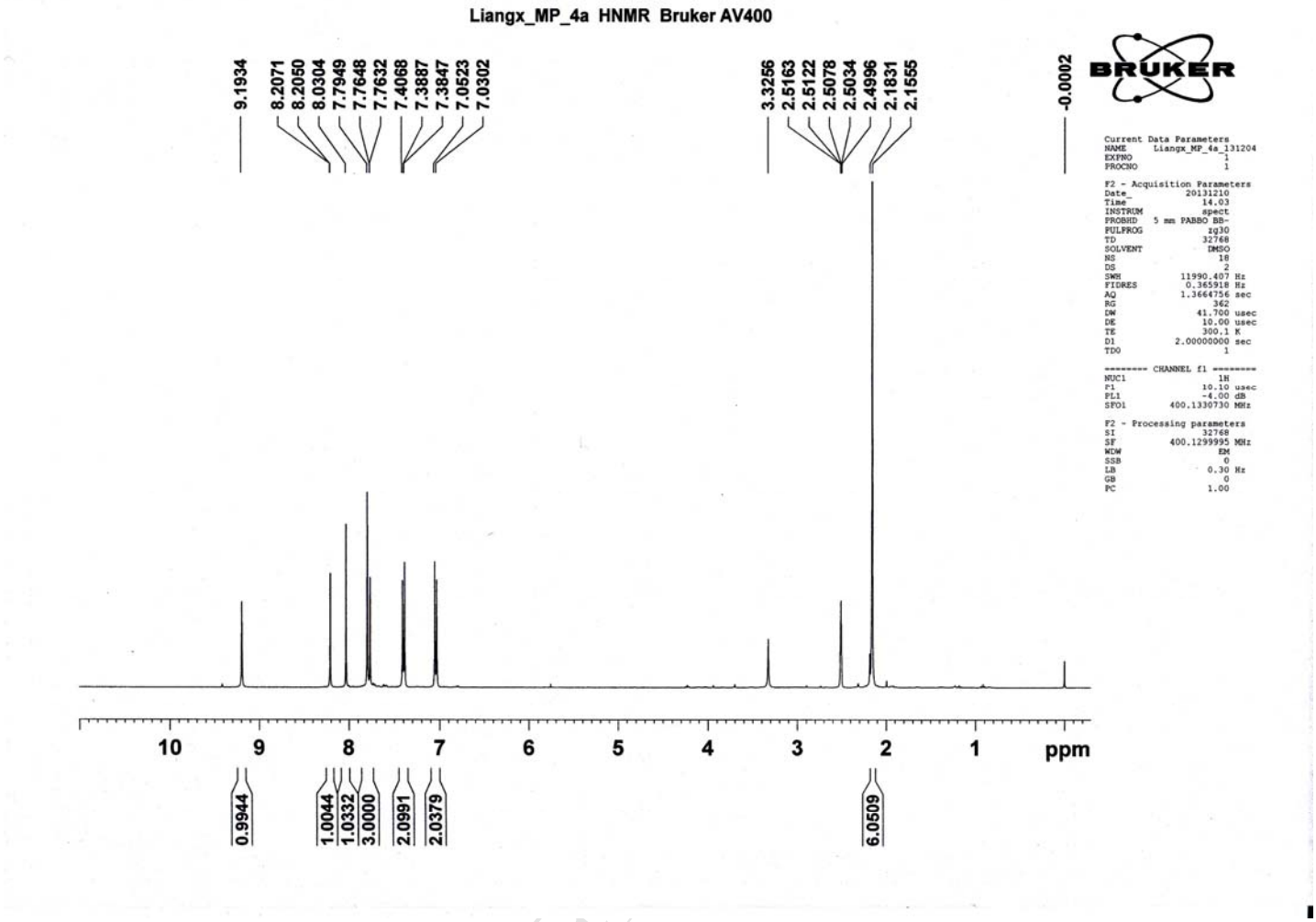

Corresponding to compound 5a (CNMR)

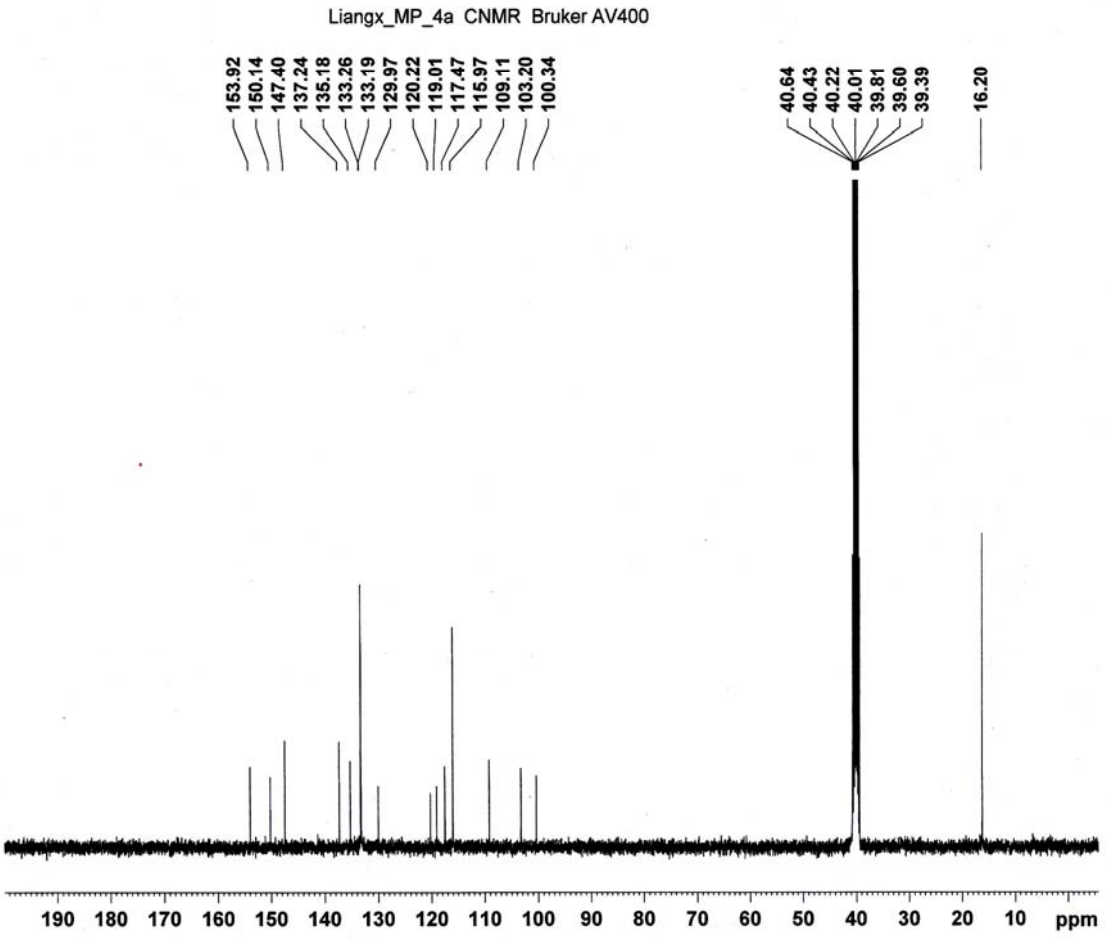

BRUKER

```
Current Data Parameters
NAME        Liangx_MP_4a_131204
EXPNO                         2
PROCNO                        1

F2 - Acquisition Parameters
Date_              20131210
Time                  13.56
INSTRUM               spect
PROBHD   5 mm PABBO BB-
PULPROG             zgpg30
TD                   65536
SOLVENT               DMSO
NS                     880
DS                       4
SWH               23980.814 Hz
FIDRES            0.365918 Hz
AQ                1.3664756 sec
RG                     26008
DW                  20.850 usec
DE                   8.00 usec
TE                   300.0 K
D1              2.00000000 sec
d11             0.03000000 sec
DELTA           1.89999998 sec
TD0                      12

======== CHANNEL f1 ========
NUC1                    13C
P1                   8.30 usec
PL1                  -3.00 dB
SFO1           100.6228298 MHz

======== CHANNEL f2 ========
CPDPRG2             waltz16
NUC2                    1H
PCPD2                80.00 usec
PL12                 12.93 dB
PL13                 12.80 dB
PL2                  -1.00 dB
SFO2           400.1316005 MHz

F2 - Processing parameters
SI                      32768
SF             100.6127690 MHz
WDW                        EM
SSB                         0
LB                       1.00 Hz
GB                          0
PC                       1.40
```

Corresponding to compound 5a (MS)

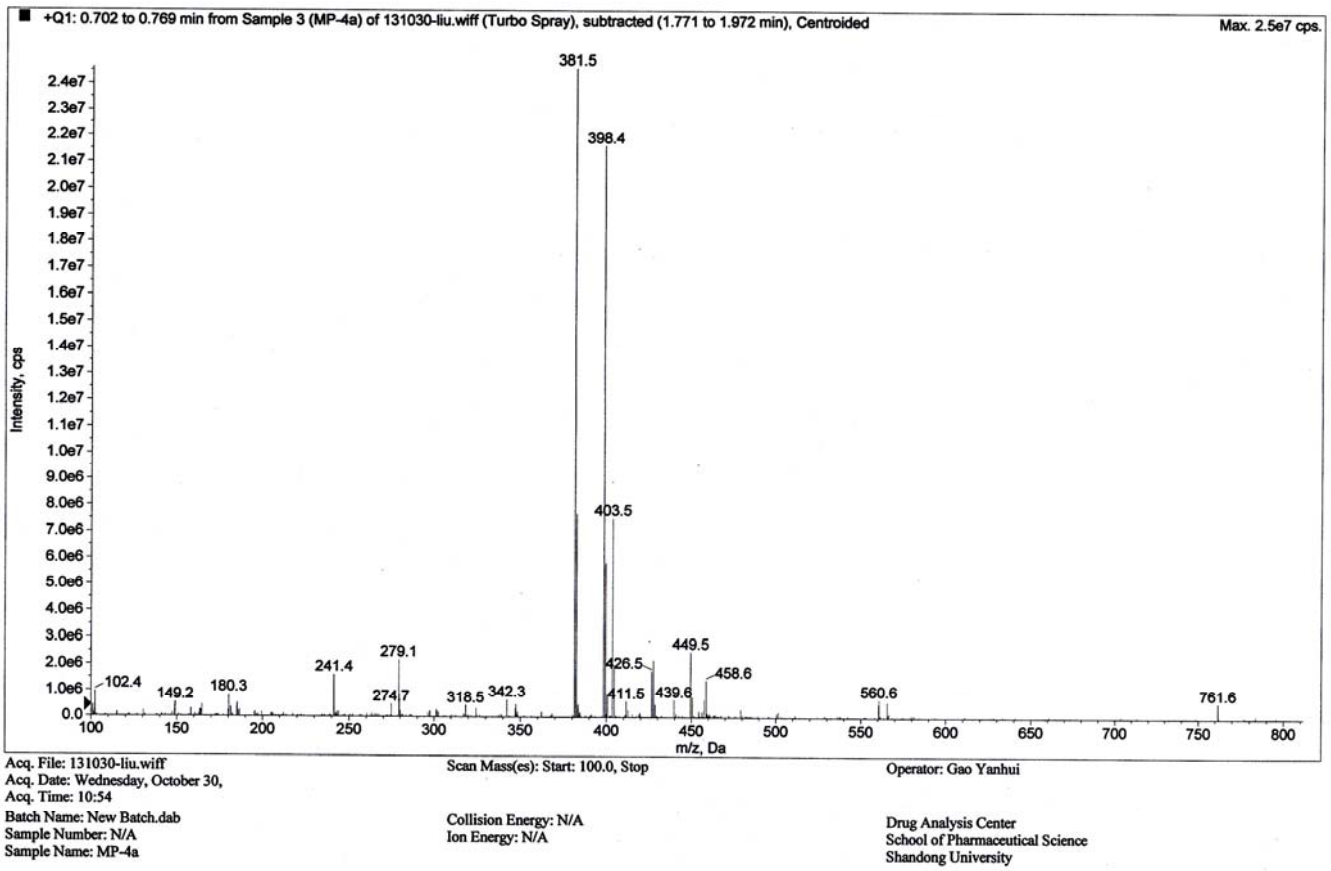

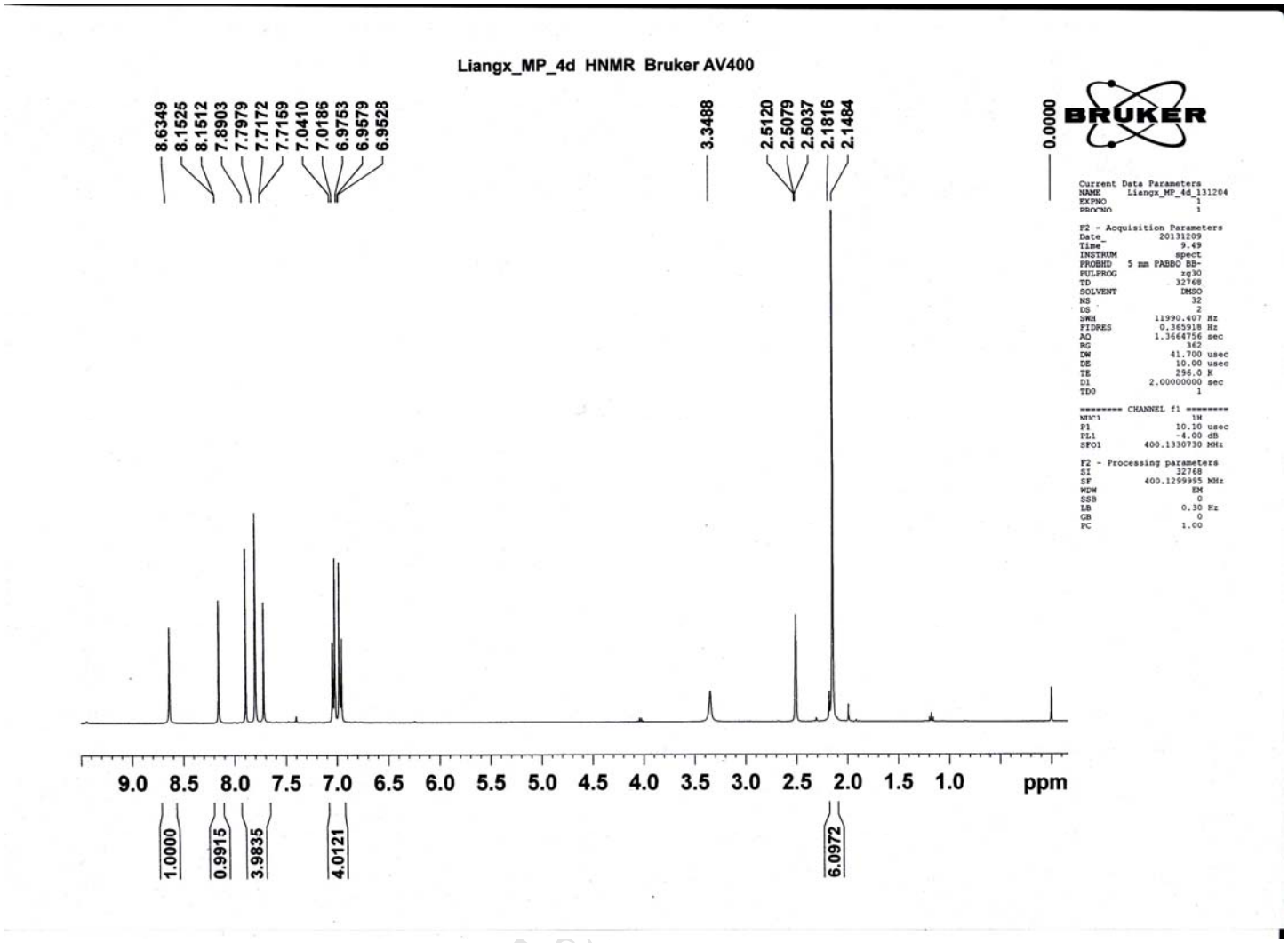
Liangx_MP_4d HNMR Bruker AV400
8.6349
8.1525
8.1512
7.8903
7.7979
7.7172
7.7159
7.0410
7.0186
6.9753
6.9579
6.9528
3.3488
2.5120
2.5079
2.5037
2.1816
2.1484
0.0000
BRUKER
Current Data Parameters
NAME Liangx_MP_4d_131204
EXPNO 1
PROCNO 1
F2 - Acquisition Parameters
Date_ 20131209
Time 9.49
INSTRUM spect
PROBHD 5 mm PABBO BB-
PULPROG zg30
TD 32768
SOLVENT DMSO
NS 32
DS 2
SWH 11990.407 Hz
FIDRES 0.365918 Hz
AQ 1.3664756 sec
RG 362
DW 41.700 usec
DE 10.00 usec
TE 296.0 K
D1 2.00000000 sec
TD0 1
======== CHANNEL f1 ========
NUC1 1H
P1 10.10 usec
PL1 -4.00 dB
SFO1 400.1330730 MHz
F2 - Processing parameters
SI 32768
SF 400.1299995 MHz
WDW EM
SSB 0
LB 0.30 Hz
GB 0
PC 1.00
9.0 8.5 8.0 7.5 7.0 6.5 6.0 5.5 5.0 4.5 4.0 3.5 3.0 2.5 2.0 1.5 1.0
ppm
1.0000
0.9915
3.9835
4.0121
6.0972

Corresponding to compound 5d (CNMR)

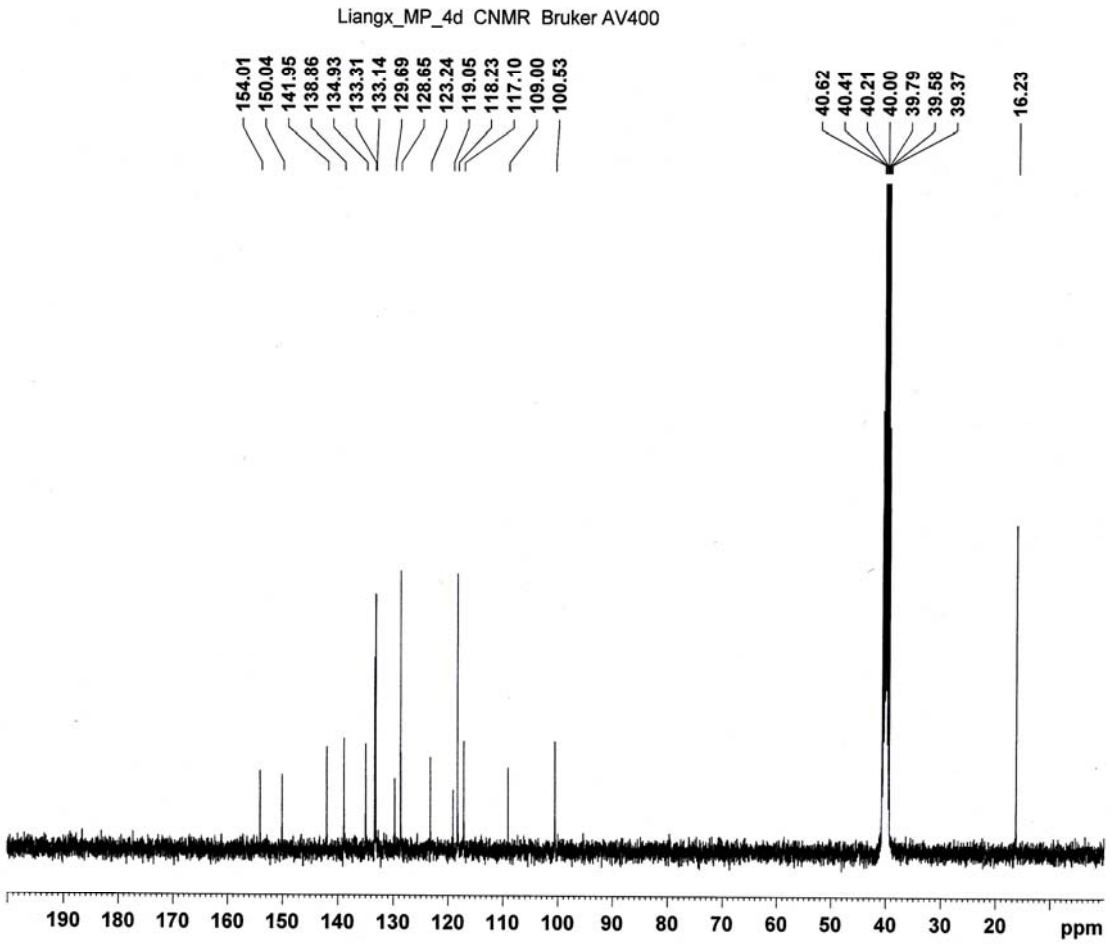

BRUKER

```
Current Data Parameters
NAME      Liangx_MP_4d_131204
EXPNO                       2
PROCNO                      1

F2 - Acquisition Parameters
Date_              20131209
Time                   9.23
INSTRUM               spect
PROBHD    5 mm PABBO BB-
PULPROG             zppg30
TD                   65536
SOLVENT               DMSO
NS                    1357
DS                       4
SWH              23980.814 Hz
FIDRES           0.365918 Hz
AQ               1.3664756 sec
RG                   29193
DW                20.850 usec
DE                 8.00 usec
TE                 297.4 K
D1             2.00000000 sec
d11            0.03000000 sec
DELTA          1.89999998 sec
TD0                     12

======== CHANNEL f1 ========
NUC1                   13C
P1                  8.30 usec
PL1                -3.00 dB
SFO1          100.6228298 MHz

======== CHANNEL f2 ========
CPDPRG2             waltz16
NUC2                    1H
PCPD2              80.00 usec
PL12               12.93 dB
PL13               12.80 dB
PL2                -1.00 dB
SFO2          400.1316005 MHz

F2 - Processing parameters
SI                     32768
SF            100.6127690 MHz
WDW                       EM
SSB                        0
LB                  1.00 Hz
GB                         0
PC                      1.40
```

Corresponding to compound 5d (MS)

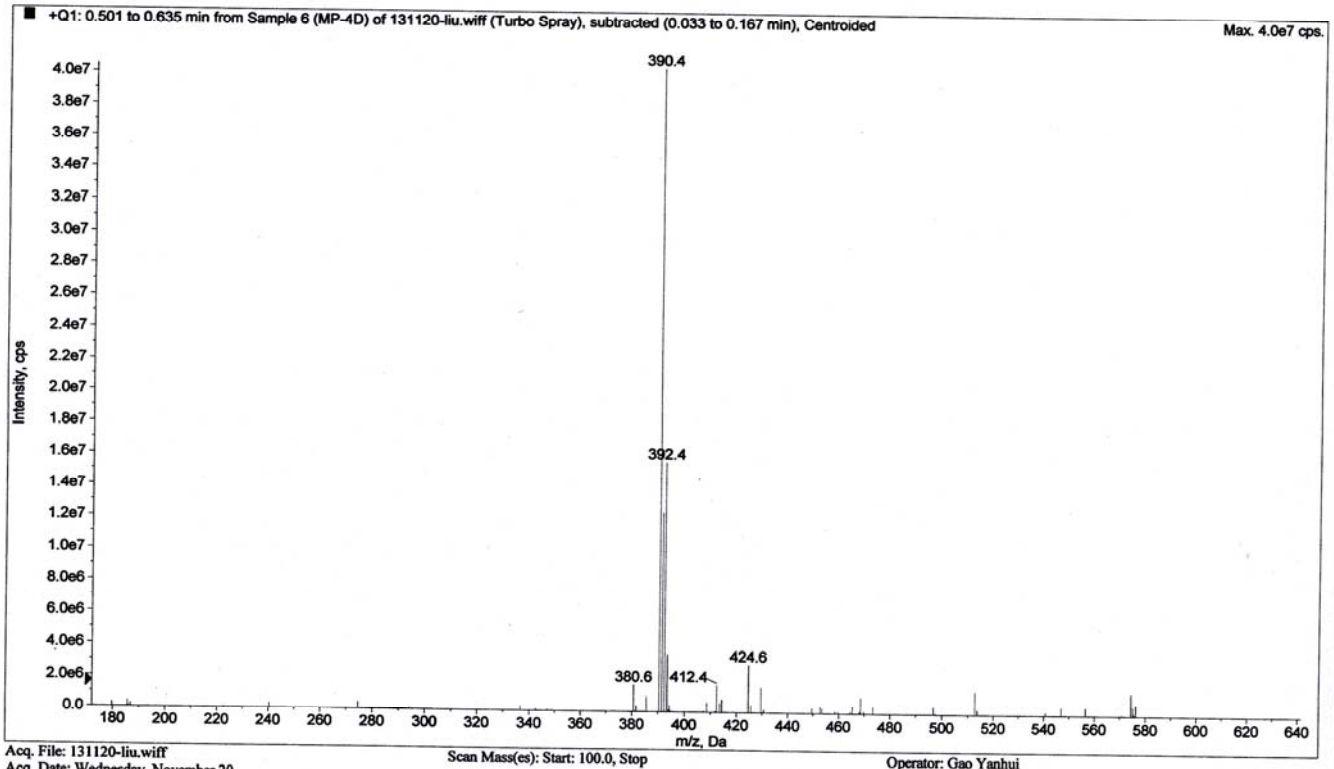

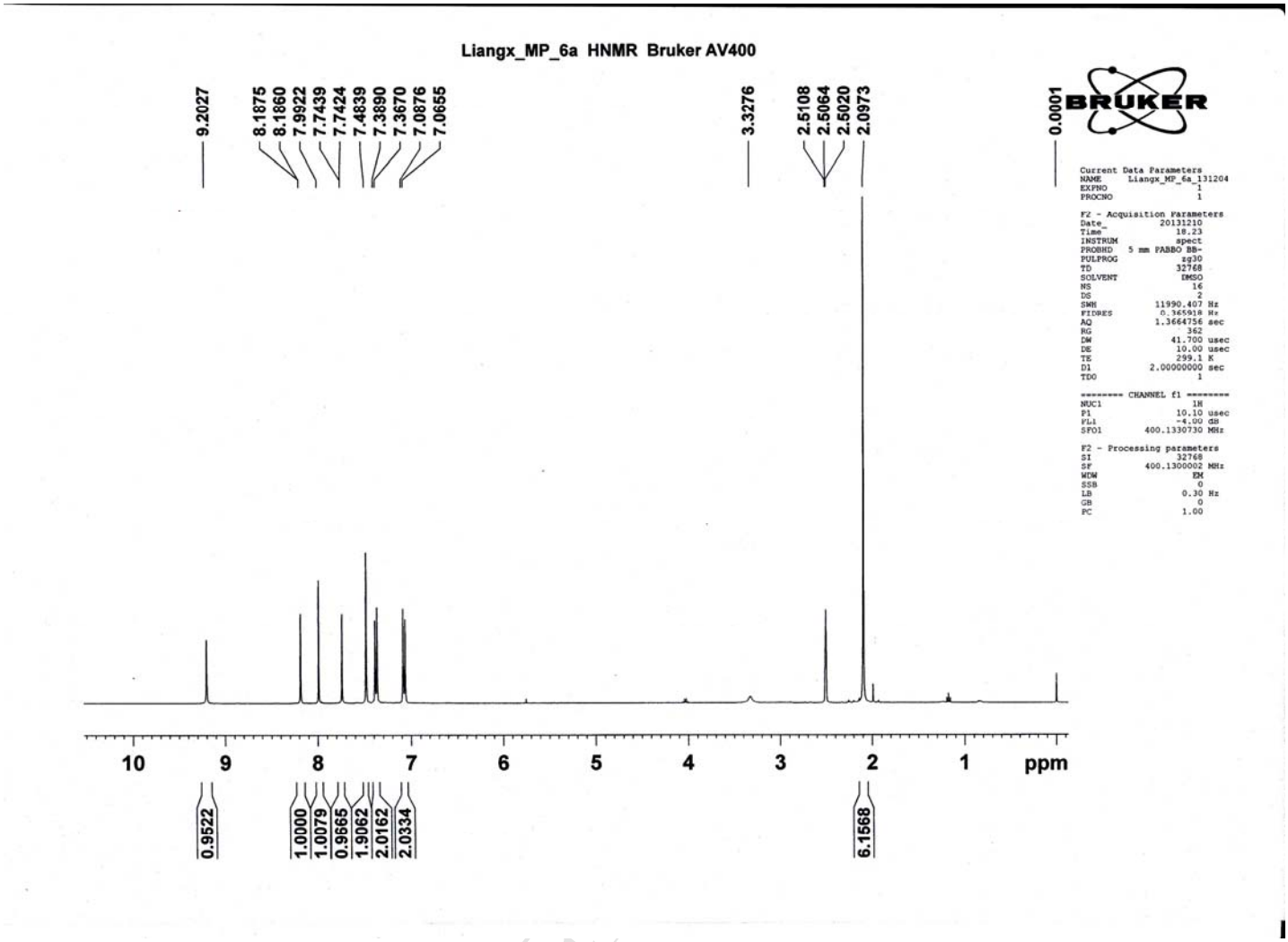
Liangx_MP_6a HNMR Bruker AV400
9.2027
8.1875
8.1860
7.9922
7.7439
7.7424
7.4839
7.3890
7.3670
7.0876
7.0655
3.3276
2.5108
2.5064
2.5020
2.0973
0.0001
BRUKER
Current Data Parameters
NAME Liangx_MP_6a_131204
EXPNO 1
PROCNO 1
F2 - Acquisition Parameters
Date_ 20131210
Time 18.23
INSTRUM spect
PROBHD 5 mm PABBO BB-
PULPROG zg30
TD 32768
SOLVENT DMSO
NS 16
DS 2
SWH 11990.407 Hz
FIDRES 0.365918 Hz
AQ 1.3664756 sec
RG 362
DW 41.700 usec
DE 10.00 usec
TE 299.1 K
D1 2.00000000 sec
TD0 1
======== CHANNEL f1 ========
NUC1 1H
P1 10.10 usec
PL1 -4.00 dB
SFO1 400.1330730 MHz
F2 - Processing parameters
SI 32768
SF 400.1300002 MHz
WDW EM
SSB 0
LB 0.30 Hz
GB 0
PC 1.00
10
9
8
7
6
5
4
3
2
1
ppm
0.9522
1.0000
1.0079
0.9665
1.9062
2.0162
2.0334
6.1568

Corresponding to compound 7a (CNMR)

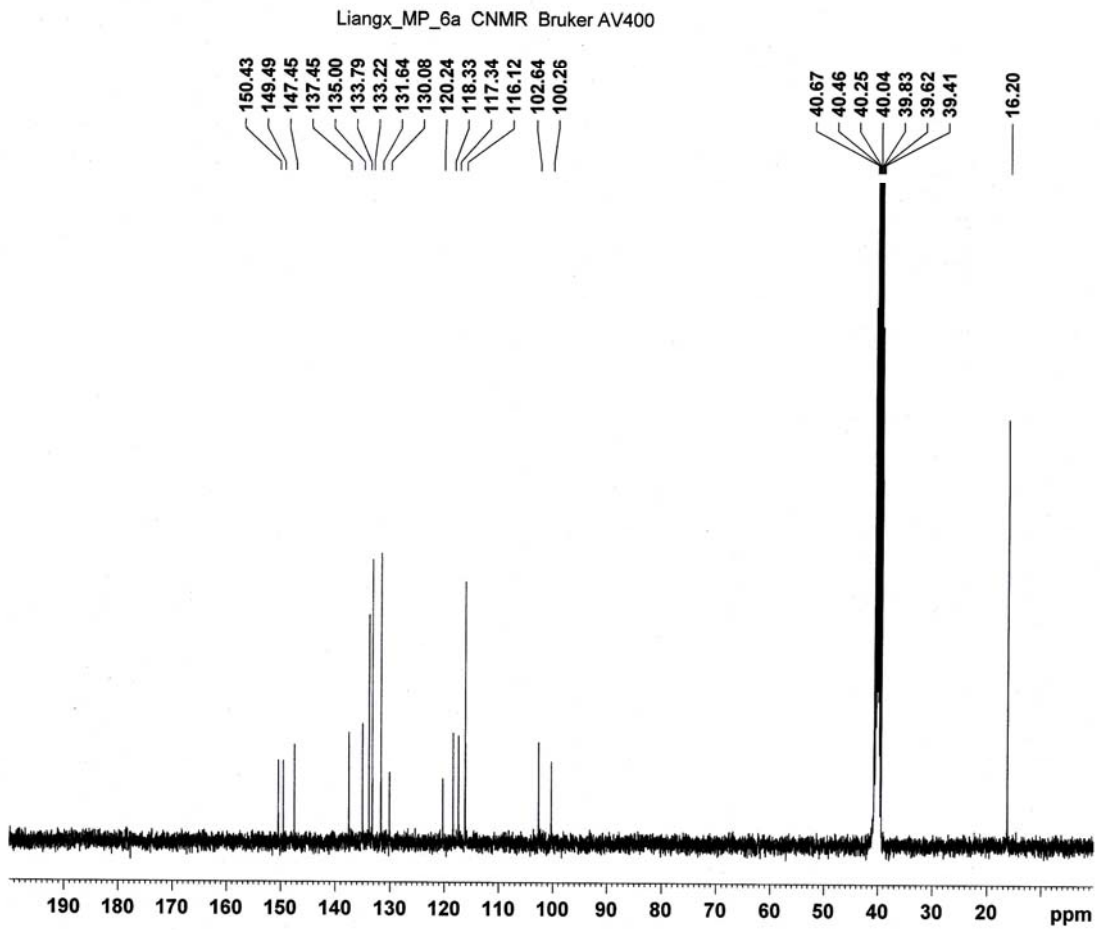

BRUKER

```
Current Data Parameters
NAME      Liangx_MP_6a_131204
EXPNO                       2
PROCNO                      1

F2 - Acquisition Parameters
Date_              20131210
Time_                 19.22
INSTRUM                spect
PROBHD   5 mm PABBO BB-
PULPROG             zgpg30
TD                   65536
SOLVENT               DMSO
NS                     1259
DS                        4
SWH              23980.814 Hz
FIDRES           0.365918 Hz
AQ               1.3664756 sec
RG                 23170.5
DW                  20.850 usec
DE                   8.00 usec
TE                  299.3 K
D1               2.00000000 sec
d11              0.03000000 sec
DELTA            1.89999998 sec
TD0                       12

======== CHANNEL f1 ========
NUC1                    13C
P1                     8.30 usec
PL1                   -3.00 dB
SFO1           100.6228298 MHz

======== CHANNEL f2 ========
CPDPRG2              waltz16
NUC2                    1H
PCPD2                 80.00 usec
PL12                  12.93 dB
PL13                  12.80 dB
PL2                   -1.00 dB
SFO2           400.1316005 MHz

F2 - Processing parameters
SI                     32768
SF           100.6127690 MHz
WDW                       EM
SSB                        0
LB                      1.00 Hz
GB                         0
PC                      1.40
```

Corresponding to compound 7a (MS)

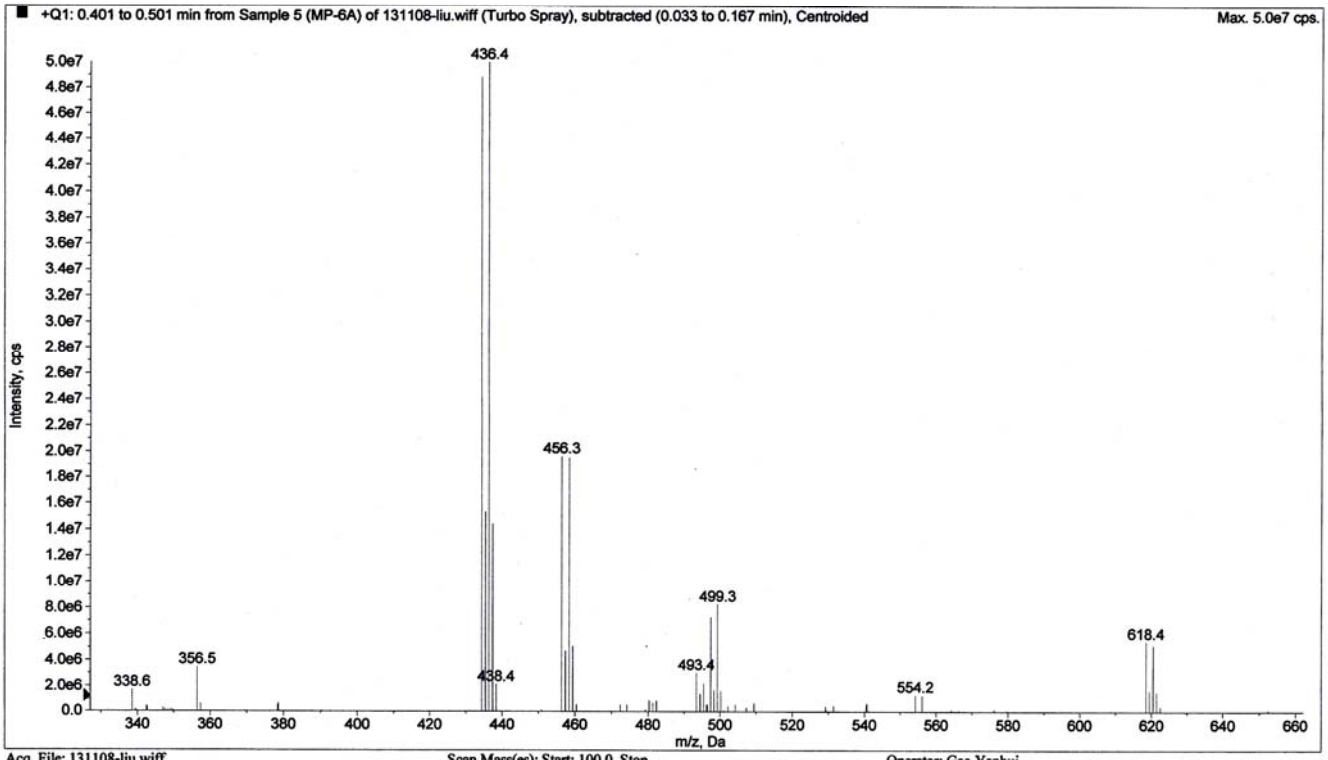

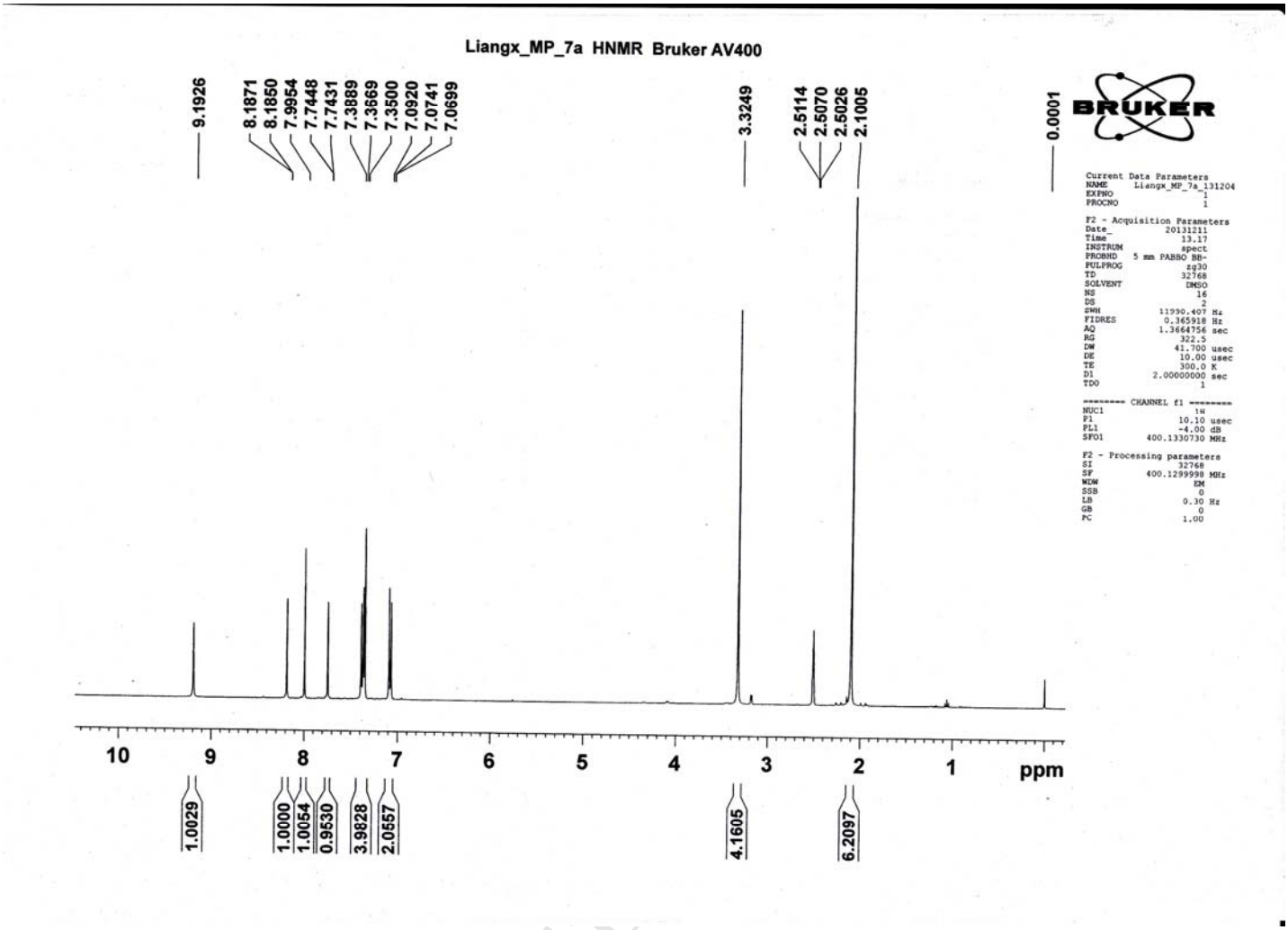

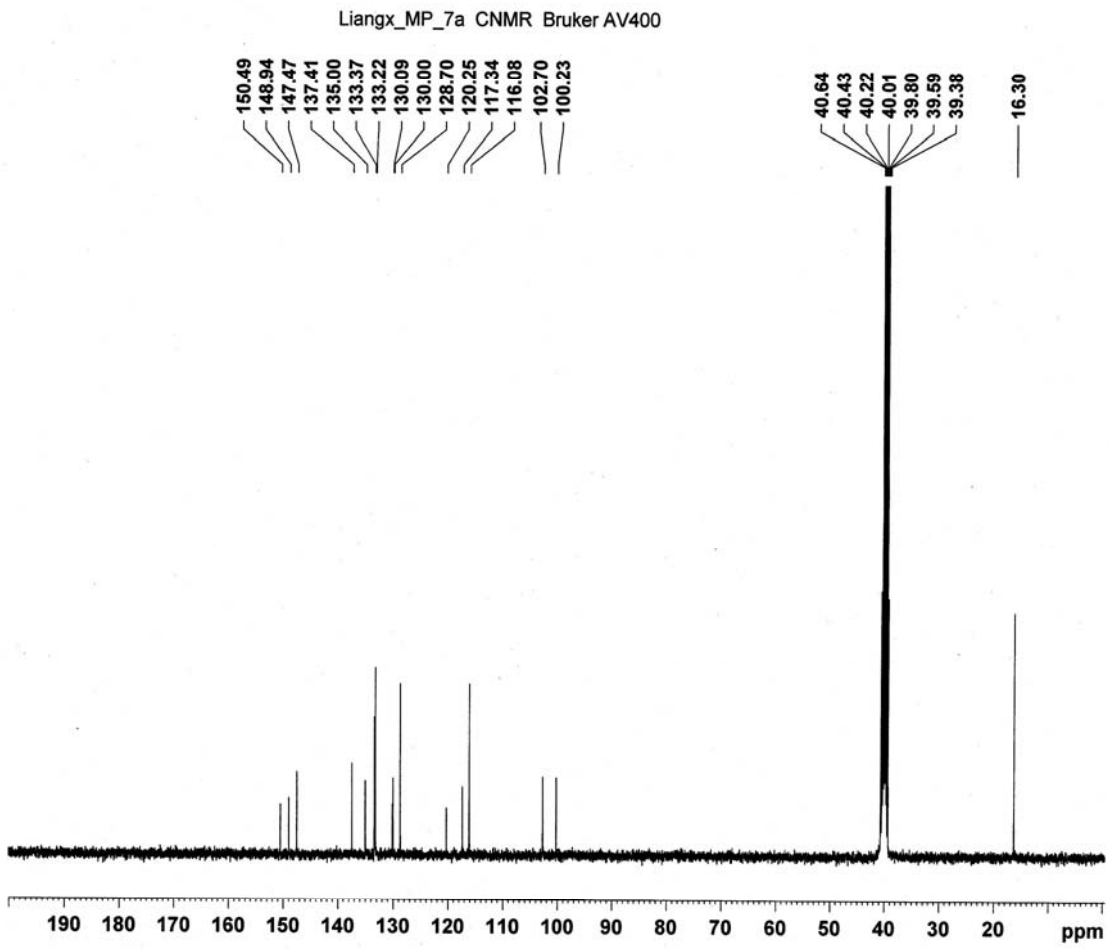

BRUKER

```
Current Data Parameters
NAME        Liangx_MP_7a_131204
EXPNO                         2
PROCNO                        1

F2 - Acquisition Parameters
Date_                  20131211
Time                      13.02
INSTRUM                   spect
PROBHD    5 mm PABBO BB-
PULPROG                 zgpg30
TD                       65536
SOLVENT                   DMSO
NS                        1264
DS                           4
SWH                  23980.814 Hz
FIDRES               0.365918 Hz
AQ                   1.3664756 sec
RG                     20642.5
DW                    20.850 usec
DE                     8.00 usec
TE                     300.0 K
D1                   2.00000000 sec
d11                  0.03000000 sec
DELTA                1.89999998 sec
TD0                          12

======== CHANNEL f1 ========
NUC1                        13C
P1                        8.30 usec
PL1                      -3.00 dB
SFO1                100.6228298 MHz

======== CHANNEL f2 ========
CPDPRG2                 waltz16
NUC2                        1H
PCPD2                    80.00 usec
PL12                     12.93 dB
PL13                     12.80 dB
PL2                      -1.00 dB
SFO2                400.1316005 MHz

F2 - Processing parameters
SI                       32768
SF                  100.6127690 MHz
WDW                         EM
SSB                          0
LB                        1.00 Hz
GB                           0
PC                        1.40
```

Corresponding to compound 8a (MS)